


RESEARCH ARTICLE

Modelling surface-water depression storage in a Prairie Pothole Region

Lauren Hay¹  | Parker Norton² | Roland Viger³  | Steven Markstrom¹ |
R. Steven Regan¹ | Melanie Vanderhoof⁴

¹U.S. Geological Survey (USGS), Box 25046, MS 412 Lakewood, Colorado, USA

²USGS, South Dakota Water Science Center, Rapid City, South Dakota, USA

³USGS, Lakewood, Boulder, Colorado, USA

⁴USGS, Geosciences and Environmental Change Center, Lakewood, Colorado, USA

Correspondence

Lauren Hay, U.S. Geological Survey (USGS), Box 25046, MS 412 Lakewood, Colorado, USA.

Email: lhay@usgs.gov

Abstract

In this study, the Precipitation-Runoff Modelling System (PRMS) was used to simulate changes in surface-water depression storage in the 1,126-km² Upper Pipestem Creek basin located within the Prairie Pothole Region of North Dakota, USA. The Prairie Pothole Region is characterized by millions of small water bodies (or surface-water depressions) that provide numerous ecosystem services and are considered an important contribution to the hydrologic cycle. The Upper Pipestem PRMS model was extracted from the U.S. Geological Survey's (USGS) National Hydrologic Model (NHM), developed to support consistent hydrologic modelling across the conterminous United States. The Geospatial Fabric database, created for the USGS NHM, contains hydrologic model parameter values derived from datasets that characterize the physical features of the entire conterminous United States for 109,951 hydrologic response units. Each hydrologic response unit in the Geospatial Fabric was parameterized using aggregated surface-water depression area derived from the National Hydrography Dataset Plus, an integrated suite of application-ready geospatial datasets. This paper presents a calibration strategy for the Upper Pipestem PRMS model that uses normalized lake elevation measurements to calibrate the parameters influencing simulated fractional surface-water depression storage. Results indicate that inclusion of measurements that give an indication of the change in surface-water depression storage in the calibration procedure resulted in accurate changes in surface-water depression storage in the water balance. Regionalized parameterization of the USGS NHM will require a proxy for change in surface-storage to accurately parameterize surface-water depression storage within the USGS NHM.

KEYWORDS

model calibration, National Hydrologic Model (NHM), North Dakota, Prairie Potholes, Precipitation-Runoff Modelling System (PRMS)

1 | INTRODUCTION

The Prairie Pothole Region (PPR), located in the Great Plains of North America (Figure 1), is characterized by millions of small water bodies, a result of the glacial retreat that occurred roughly 13,000 years ago (Flint, 1971; Tiner, 2003). These surface-water depressions are commonly referred to as geographically isolated wetlands, although that terminology has been somewhat controversial (Mushet et al., 2015) because the connectivity of these water bodies can vary over space and time (Leibowitz & Vining, 2003; Shook, Pomeroy, &

van der Kamp, 2015; Winter & LaBaugh, 2003). For this paper, the PPR water bodies will be referred to as surface-water depressions.

The surface-water depressions in the PPR have long been known to provide an important contribution to the hydrologic cycle (Cohen et al., 2016; Eisenlohr & Sloan, 1968). Surface-water depressions can collect and store precipitation and surface runoff (De Laney, 1995; Ludden, Frink, & Johnson, 1983) resulting in reduced (or delayed) runoff that reaches the stream channels and reduced peak streamflow (Philips, Spence, & Pomeroy, 2011; Shaw, Vanderkamp, Conly, Pietroniro, & Martz, 2012; Vanderhoof, Alexander, & Todd, 2015).

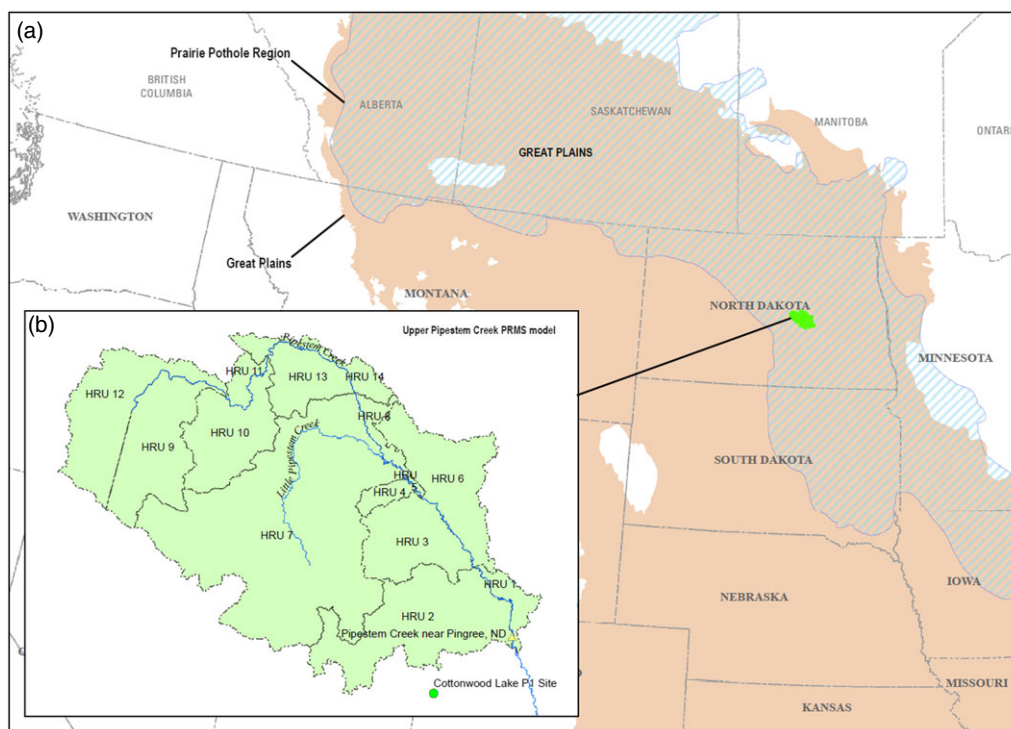


FIGURE 1 (a) Location of the Upper Pipestem Creek basin (green-shaded area) within the Great Plains (tan-shaded area) and the Prairie Pothole Region (blue solid lines) and (b) the hydrologic response units (HRUs) within the National Hydrologic Modelling framework for the Upper Pipestem Creek basin and the location of the Cottonwood Lake P1 site (green dot). PRMS = Precipitation-Runoff Modelling System

The U.S. Environmental Protection Agency (2015) has concluded that research on the frequency, magnitude, timing, duration, and rate of fluxes from surface-water depressions is needed to improve the Environmental Protection Agency's abilities to "identify waters of national importance and maintain the long-term sustainability and resiliency of valued water resources." The aggregated hydrologic effects of surface-water depression storage can be examined using process-based watershed-scale hydrologic models (Golden et al., 2014). Including these relatively fine-scale geographic features is an important step in the development of a scientifically valid national hydrological modelling system and for supporting effective natural resource management (Viger, Hay, Jones, & Buell, 2010).

For this study, the Precipitation-Runoff Modelling System (PRMS) was used to simulate changes in surface-water depression storage in the 1,126-km² Upper Pipestem Creek basin located within the PPR of North Dakota, USA (Figure 1). The PRMS Upper Pipestem Creek model was extracted from the U.S. Geological Survey's (USGS) National Hydrologic Model (NHM), which was developed to support coordinated, comprehensive, and consistent hydrologic model development and application across the conterminous United States (CONUS; Regan et al., 2018). This CONUS-scale application of PRMS uses a "lumped" configuration of the surface-water depressions within each hydrologic response unit (HRU) that prevents the cascading "fill and spill" connectivity between individual surface-water depressions within an HRU.

The HRU representation in the Soil and Water Assessment Tool model was redefined to account for individual surface-water depressions, allowing for fill and spill connectivity (Evenson, Golden, Lane, & D'Amico, 2016); however, this type of approach is not practical for

application at the CONUS-scale PRMS model due to parameterization and run time considerations. The daily time step PRMS model executes quickly, and its modular nature allows analysis of different process representations both locally and across the nation. The hydrologic simulations from the PRMS model extracted from the NHM serve as a baseline for model improvement. The default parameters (Driscoll, Markstrom, Regan, Hay, & Viger, 2017) can be improved through exploration of ancillary hydrologic information at the national, regional, and local scale.

The objective of this study was to use the Upper Pipestem Creek PRMS NHM to determine if the inclusion of ancillary hydrologic information about surface-water depression storage in model calibration improves the simulation of surface-water depression storage dynamics and streamflow simulation. Lake elevations from the nearby Cottonwood P1 site (Figure 1) were used as a proxy for change in surface depression storage. Two model calibration strategies were evaluated: a strategy that calibrated PRMS parameters to (a) a water balance and components of the daily hydrograph and (b) a water balance, components of the daily hydrograph, and lake elevations from the Cottonwood P1 site (Figure 1) in North Dakota.

2 | STUDY AREA

The Upper Pipestem Creek basin was chosen due to its proximity to the Cottonwood Lake P1 site, a long-term wetland ecosystem monitoring site located just south of the Upper Pipestem Creek basin (Figure 2; Mushet & Euliss Jr., 2012). Lake elevation measurements from the Cottonwood Lake P1 site (Mushet, Rosenberry, Euliss Jr., &

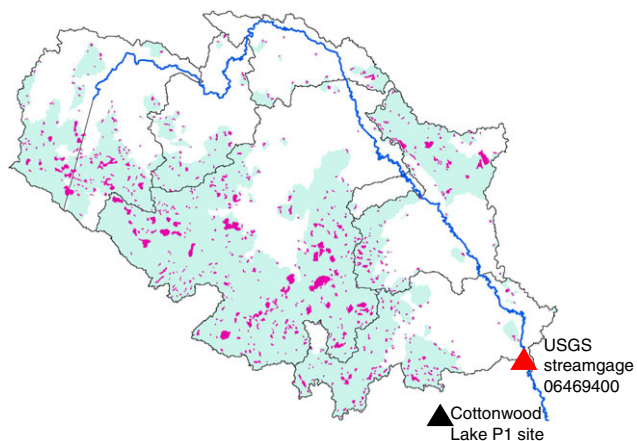


FIGURE 2 Upper Pipestem Creek basin: hydrologic response units (black lines), surface-water depression storage (magenta), contributing area to surface-water depressions (light blue shading), U.S. Geological Survey (USGS) streamgage 06469400 Pipestem Creek near Pingree, North Dakota, and location of the Cottonwood Lake P1 site with lake elevation measurements

Solensky, 2016) are considered to be a good indicator of local surface-water storage (written comm., Brian Neff, October 2015) and provide a unique opportunity to relate these measurements to surface depression storage in the Upper Pipestem Creek basin. Studies in the Cottonwood study area indicate that surface-water depressions interact with the local flow system (Winter, 2003). Interactions between depressions and groundwater vary within this area; some depression contribute to groundwater, others receive discharge of groundwater, whereas some do both.

Figure 2 shows the extent of the surface-water depressions for the Upper Pipestem Creek basin. Waterbody delineations from the National Hydrography Dataset Plus (NHDPlus; version 1.0) were used to map surface-water depressions. The magenta-shaded areas in Figure 2 represent the surface-water depressions; 3.5% of the

basin from this analysis. Because surface-water depressions are assumed to be geographically isolated from the stream network in the PPR, waterbodies that are on or extremely close to the stream were eliminated from the surface-water depression map. A 60-m buffer on either side of the stream was used to filter out waterbodies that are considered to be on-stream. The analysis relied on the 30-m digital elevation model associated with NHDPlus; therefore, the 60-m buffer is essentially two grid cells on either side of the stream. The light blue-shaded areas in Figure 2 represent the surface runoff contributing areas for the depressions; 48% of the basin from this analysis. This is in contrast to the USGS National Water Information System (NWIS) description for USGS streamgage 06469400 Pipestem Creek near Pingree, North Dakota, which indicates that runoff from 37% of the drainage basin upstream from the streamgage contributes to streamflow, whereas runoff for 63% of the drainage basin stays within the basin, not contributing to the total basin streamflow (https://waterdata.usgs.gov/nwis/inventory/?site_no=06469400&agency_cd=USGS).

2.1 | Climate

Figure 3a–c shows the range in mean daily minimum and maximum temperature and precipitation by month for the Upper Pipestem Creek basin. The climate data used in this study are derived from the Daymet version 2 dataset (Thornton et al., 2014); a 1-km gridded product that provides daily values of precipitation and minimum and maximum temperature interpolated and extrapolated from the Global Historical Climatology Network (Menne, Imke, Vose, Gleason, & Housaon, 2012) daily surface observations (Thornton, Running, & White, 1997). The accuracy of the Daymet data in the Upper Pipestem Creek basin is dependent on the interpolation methodology and the accuracy of the Global Historical Climatology Network surface observations in the vicinity.

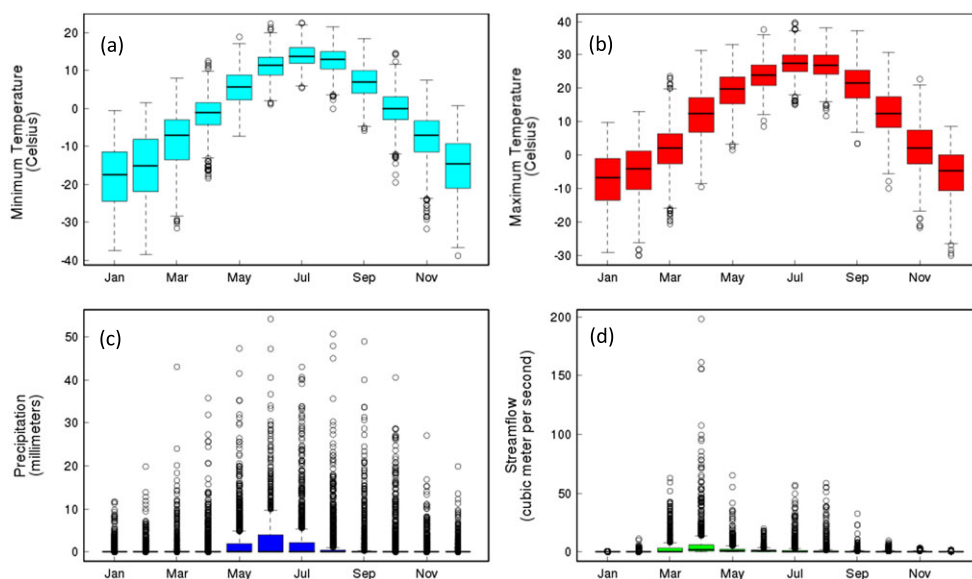


FIGURE 3 Mean daily (1980–2014): (a) minimum temperature; (b) maximum temperature; (c) precipitation; and (d) streamflow for the Upper Pipestem Creek basin by month

2.2 | Streamflow

Figure 3d shows the range in mean daily streamflow by month for Pipestem Creek near Pingree, North Dakota (USGS streamgage 06469400), and Figure 4a,b shows plots of daily mean streamflow generated by the NWIS (U.S. Geological Survey, 2016). In general, the quality of streamflow records for this streamgage is considered “fair,” except for the estimated daily discharges, which are considered “poor.” A fair rating indicates that about 85% of the daily discharges are within 15% of the true value, and a poor rating indicates that daily discharges have less than fair accuracy (Kennedy, 1983); indicating caution when using this dataset for model calibration and/or evaluation.

Figure 4a,b shows NWIS-generated daily hydrographs for streamgage 06469400 for water years (WYs) 1975–2014 (Figure 4a) and WY 1996 (inset; Figure 4b). Figure 4c shows the corresponding flow

duration curve. Note the large portion of the record with zero, or close to zero, streamflow. In general, December through March streamflow is estimated (considered poor) due to ice interfering with streamgage measurements, beginning in WY 1990 (red lines; Figure 4a), which brings into question the quality of the record prior to WY 1990—Was there really no ice prior to WY 1990? This may correspond to changes in NWIS capability around this time; estimate flags may exist in the paper record prior to WY 1990.

3 | METHODS

The following sections describe the hydrologic model configuration and the multiple-objective, step-wise, automated calibration procedures.

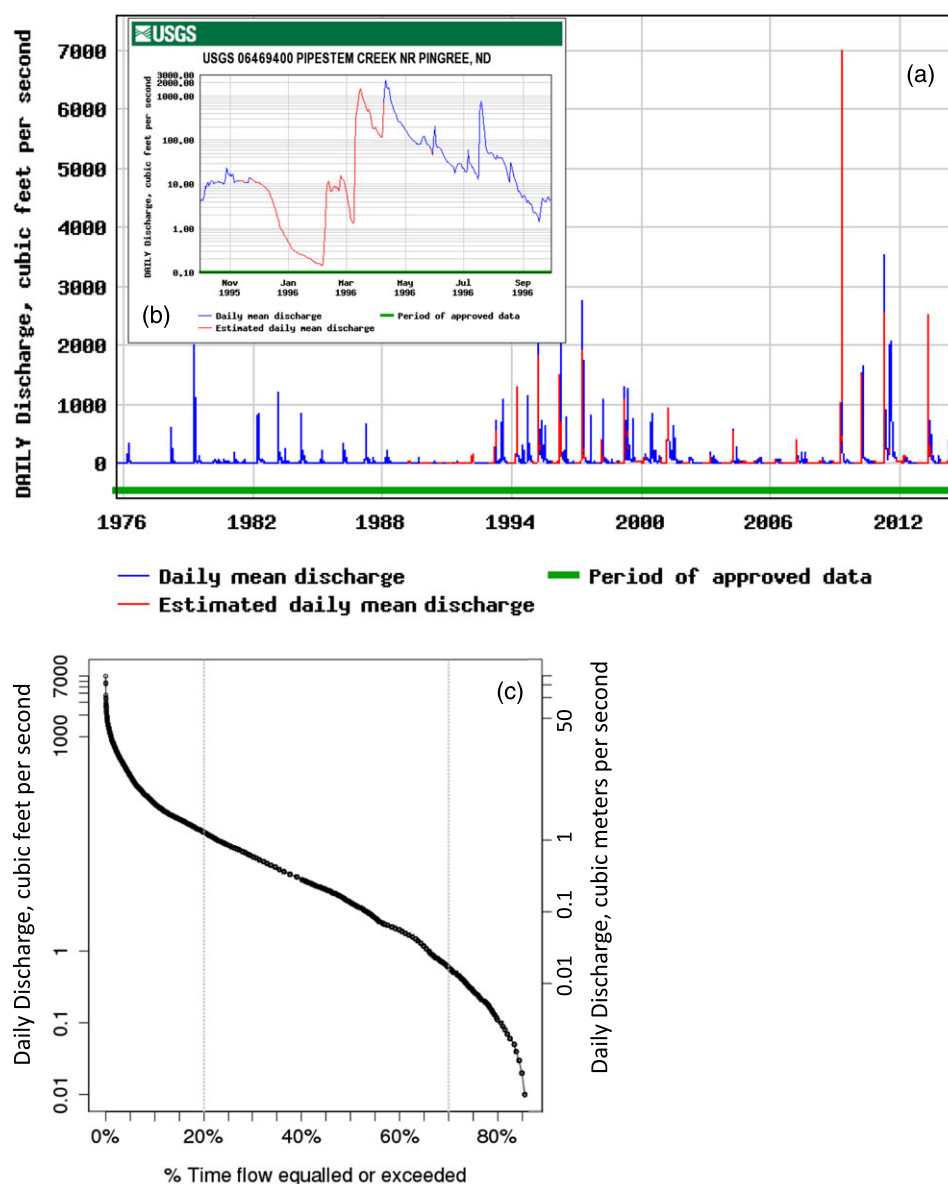


FIGURE 4 Streamflow (discharge) record for U.S. Geological Survey (USGS) streamgage 06469400 (Pipestem Creek near Pingree, North Dakota): (a) water years 1975–2014; (b) water year 1996 (http://waterdata.usgs.gov/usa/NWIS/uv?site_no=06469400); and (c) flow duration curve (note that units are shown in cubic feet per second to be consistent with the National Water Information System). A water year is the 12-month period of October 1 through September 30 designated by the calendar year in which it ends

3.1 | Hydrologic model configuration

The PRMS model (Markstrom et al., 2015) was used to simulate the effects of surface depression storage on watershed response in the Upper Pipestem Creek basin. PRMS is a modular, deterministic, distributed-parameter, physical-process watershed modelling system used to simulate streamflow by process algorithms that are based on a physical law or empirical relation with measured or estimated characteristics (Figure 5a). Distributed parameter capabilities are provided by partitioning the study basin into HRUs in which the components of

flow (groundwater flow [groundwater reservoir], interflow [gravity reservoir], and surface run-off [impervious and capillary reservoirs]) are computed in response to precipitation, air temperature, and land surface and subsurface dynamics (Figure 5a). Daily maximum and minimum temperature and precipitation data from the gridded Daymet version 2 dataset (Thornton et al., 2014) were used for PRMS climate forcings. For this study, the gridded Daymet climate data were spatially aggregated to the model HRUs using an area-weighted averaging algorithm using the USGS Geo Data Portal (Blodgett, Booth, Kunicki, Walker, & Viger, 2011).

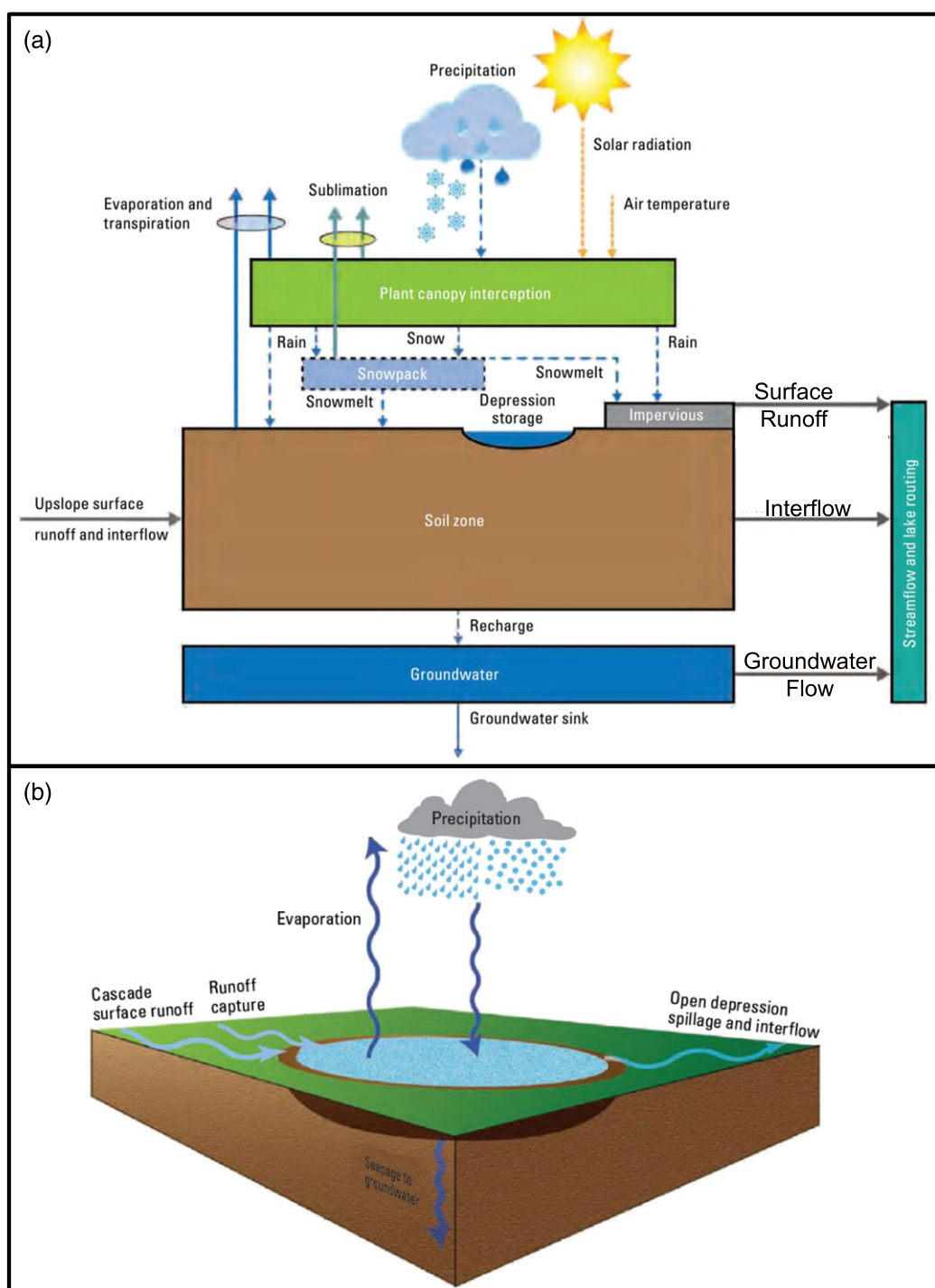


FIGURE 5 Precipitation-Runoff Modelling System conceptualization: (a) basin components and fluxes and (b) surface-water depression storage processes (adapted from Regan & LaFontaine, 2017)

3.1.1 | NHM

The USGS NHM default parameters are documented in Regan et al. (2018) and archived in Driscoll et al. (2017). The Geospatial Fabric database (Viger & Bock, 2014), created for the USGS NHM, contains the hydrologic modelling units (HRUs and stream segments) and parameter values derived from datasets that characterize the physical features of the entire CONUS for 109,951 HRUs. This HRU configuration is based on an aggregation of the NHDPlus dataset (<https://www.epa.gov/waterdata/nhdplus-national-hydrography-dataset-plus>), an integrated suite of geospatial data that incorporates features from the National Hydrography Dataset (U.S. Geological Survey, 2007–2014), the National Elevation Dataset (<https://lta.cr.usgs.gov/NED>), the National Land Cover Dataset (Homer et al., 2007), and the Watershed Boundary Dataset (<https://nhd.usgs.gov/wbd.html>). PRMS models can be spatially subsetting from the USGS NHM for local applications, resulting in stand-alone local PRMS models that can be calibrated and customized for a particular study area (Regan et al., 2018). For this study, the PRMS model for the Upper Pipestem Creek basin was extracted from the USGS NHM; consisting of 14 HRUs for an area of 1,126 km² (Figure 1b).

3.1.2 | Surface depression storage

The PRMS utilizes a lumped surface depression representation for each HRU, which is valuable where surface depressions are too small

or numerous to conveniently model as discrete spatial units, but where the aggregated storage capacity of these units is large enough to have an effect on streamflow (Viger et al., 2010). Vining (2002), Viger et al. (2010), Viger, Hay, Markstrom, Jones, and Buell (2011), and LaFontaine, Hay, Viger, Regan, and Markstrom (2015) showed the value of including surface depression storage in PRMS streamflow simulations. Figure 5b shows the conceptualization of the surface-water depression storage processes in the PRMS for one HRU.

The data and methodology used to estimate HRU surface depression storage capacity were derived for the USGS NHM using NHDPlus (version 1.0) waterbodies. The parameters associated with surface depression storage are described in appendix 1 and table 1.3 of the PRMS manual (Markstrom et al., 2015). All surface depressions were considered to be open in the Upper Pipestem PRMS model, allowing for fill and spill of surface depressions in each HRU. Note that the fill and spill terminology used here is with respect to the context of the PRMS parameterization technique. Leibowitz and Vining (2003) characterized the fill and spill dynamics in the PPR as pulsed surface-water connections limited to periods following spring snow melt (Figure 6a). Figure 6b demonstrates what researchers (Barton, Herczeg, Dahlhaus, & Cox, 2013; Huang, Dahal, Young, Chander, & Liu, 2011; Leibowitz et al., 2016) refer to as “fill and merge” dynamics; a nearly continuous surface-water connection. Figure 6c conceptualizes surface depression connectivity for a rectangular bottom depression for a PRMS HRU. The PRMS depression storage essentially behaves as fill and merge,

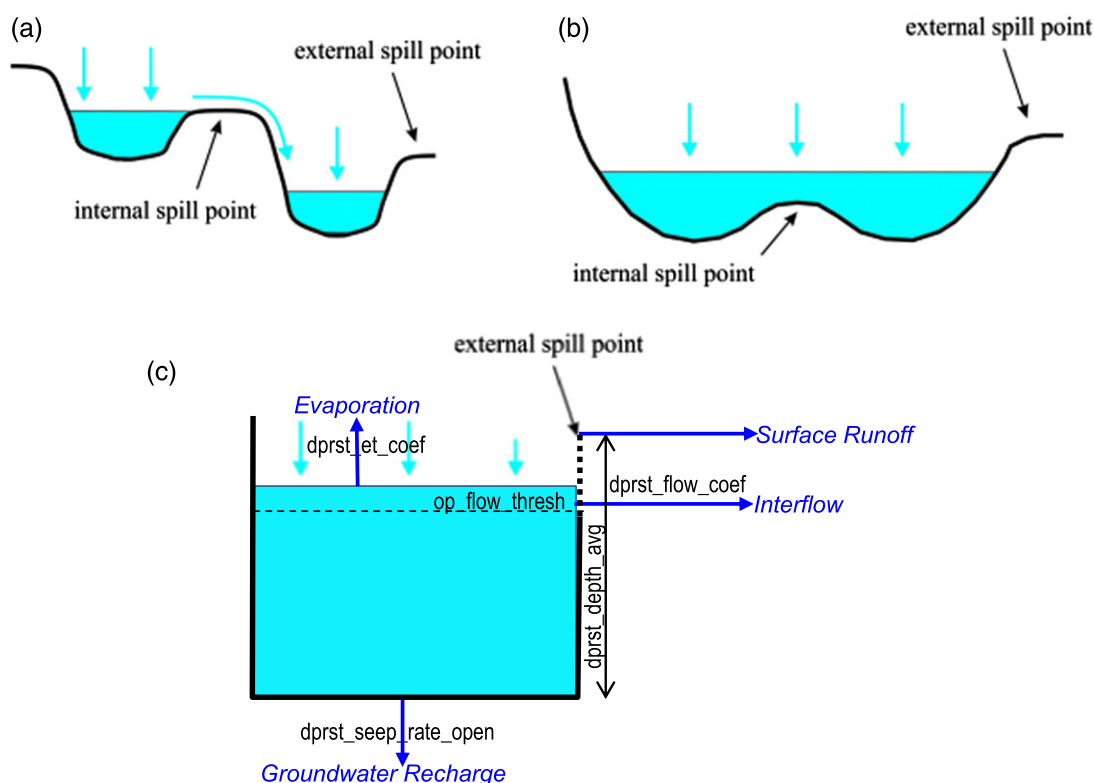


FIGURE 6 Waterbody connectivity: (a) “fill and spill” and (b) “fill and merge” (from Leibowitz, Mushet, & Newton, 2016) versus (c) “merge, fill, and spill”; the Precipitation-Run-off Modelling System conceptualization for rectangular bottom surface-water depression. Relevant Precipitation-Run-off Modelling System parameters are as follows: dprst_et_coef (fraction of unsatisfied potential evapotranspiration); dprst_seep_rate_open (used in linear seepage flow equation); dprst_flow_coef (used in linear flow routing equation); op_flow_thresh (fraction of depression storage above which surface run-off occurs; any water above maximum open storage capacity spills as surface run-off); and dprst_depth_avg (average depth of storage depressions at maximum storage capacity)

with fill and spill limited to periods of excessive storage (based on the `dprst_dept_avg` parameter [average depth of the surface-water depression storage at maximum storage capacity for each HRU; Figure 6c]) making it more of a “merged, fill, and spill” conceptualization. Fill and merge can contribute to streamflow, expanding and merging with a stream-intersect wetland (Vanderhoof, Christensen, & Alexander, 2016). As noted by Leibowitz et al. (2016), fill and spill leads to more streamflow out of the basin, whereas fill and merge results in more internal basin storage.

In PRMS, the surface depressions are “full” when the external spill point is reached (Figure 6c). This means that the aggregate surface-water depression storage volume for an HRU is full in the merged, fill, and spill conceptualization. Portions of surface depression storage in an HRU may physically be full and spill to the land surface, but spillage in PRMS is considered to be only the water that spills to the stream network. The merged concept allows for internal capture within an HRU and spillage to the stream network as a lumped process. Additional water may flow to the stream network as a portion of groundwater flow that has seeped from depression storage. Water storage in the surface-water depression storages is reduced by actual evapotranspiration at an adjusted potential evapotranspiration rate on the basis of surface area and available water of the surface-water depression storage within an HRU.

3.2 | Hydrologic model calibration

The traditional approach to calibration and evaluation of hydrologic models—comparison of observed and simulated streamflow—is not sufficient by itself in model calibration and evaluation (Refsgaard, 1997). Intermediate process variables computed by the hydrologic model could be characterized by parameter values that do not accurately represent those hydrological processes in the physical system (Hay & Umemoto, 2007). In answer to this, many modellers now examine the intermediate process variables in addition to streamflow with calibration datasets when there is an associated “observed” variable that can be used for calibration. For example, additional calibration datasets such as potential evapotranspiration and solar radiation (Hay, Leavesley, & Clark, 2006), snow-covered area (Franz & Karsten, 2013; Hay, Leavesley, Clark, Markstrom, et al., 2006; Isenstein, Wi, & Yang, 2015), snow water equivalent (Bock, Hay, McCabe, Markstrom, & Atkinson, 2016), soil moisture (Campo, Caparrini, & Castelli, 2006; Koren, Moreda, & Smith, 2008; Santanello et al., 2007; Thorstensen, Nguyen, Hsu, & Sorooshian, 2016; Wanders, Karssenbergh, de Roo, de Jong, & Bierkens, 2014; Zamora, Clark, Rogers, Ek, & Lahmers, 2014), and evapotranspiration (Cao et al., 2006; Immerzeel & Droogers, 2008; Rientjes, Muthuwatta, Bos, Booij, & Bhatti, 2013) have been used as additional controls or targets within the model calibration process.

The Upper Pipestem Creek basin provides a unique opportunity for model calibration by using lake (surface water) elevation measurements from the nearby Cottonwood Lake P1 site (Figure 1; Mushet et al., 2016) as a proxy to calibrate surface depression storage. The Cottonwood Lake P1 site is a small, shallow wetland, seldom deeper than 1 m and, at that depth, with a surface area of approximately 2,000 m² (Parkhurst, Sturrock, Rosenberry, & Winter, 1995). Discontinuous lake elevation measurements are available for the Cottonwood

Lake P1 site that date back to 1980 (Figure 7), with no recorded measurements in the winter when the lake was frozen. For this application, the lake elevation time series for the Cottonwood Lake P1 site were normalized (between 0 and 1; Equation 1; see Figure 7) as follows:

$$\text{nrmP}(i) = (P(i) - P_{\min}) / (P_{\max} - P_{\min}) \quad (1)$$

where $\text{nrmP}(i)$ is the normalized lake elevation for time i ; $P(i)$ is the lake elevation for time i ; P_{\min} is the minimum value for P ; and P_{\max} is the maximum value for P . Normalized lake elevations could then be compared by HRU to the PRMS intermediate process variable that contains the fraction of the depression storage (0 to 1) within an HRU that is filled (PRMS output variable `dprst_vol_frac`).

During the drought of 1988–92 in North Dakota (marked in grey; Figure 7), Cottonwood Lake went dry (Winter, 2003). For calibration purposes, it was assumed that everything in the vicinity was also dry (e.g., surface depression storages in all HRUs were empty; `dprst_vol_frac` = 0). It is more difficult to determine when the surface-water depression storages are full based on the lake elevation measurements from the Cottonwood P1 site; from the wetlands perspective, the upper threshold (how full it gets) may be more critical, because that is what controls spilling from surface-water depressions (written comm., Scott Leibowitz, October 2015).

The PRMS Upper Pipestem Creek basin model was calibrated using Luca, a software package developed to carry out multiple-objective, step-wise, automated calibration for the PRMS (Hay & Umemoto, 2007) using the shuffled complex evolution global search algorithm (Duan, Gupta, & Sorooshian, 1993; Duan, Sorooshian, & Gupta, 1992; Duan, Sorooshian, & Gupta, 1994). The Luca software can be set up to assure that intermediate model process variables and streamflow are simulated consistently with observed values (Hay, Leavesley, & Clark, 2006). The parameters influencing each of the selected PRMS model processes are calibrated sequentially.

Two Luca calibration procedures were evaluated: (a) a four-step methodology that calibrates parameters to the water balance and components of the daily hydrograph and (b) a five-step methodology that calibrates parameters to the water balance, components of the daily hydrograph, and the normalized lake elevations from the Cottonwood P1 site (Figure 7). Table 1 outlines the two calibration procedures, the parameters, and parameter ranges for calibration. Both calibration procedures start with the same initial parameter file containing all PRMS parameters as extracted from the USGS NHM. In each calibration step, the parameters designated in Table 1 are calibrated. These calibrated parameter values replace the respective parameter values in the parameter file; this parameter file becomes the initial parameter file for the next calibration step. Completion of the four/five calibration steps constitutes a round. Once a parameter is calibrated, it does not change for the remainder of that calibration round. This process is repeated until no further improvement in model performance is seen (four rounds for each of the two calibration procedures).

Markstrom, Hay, and Clark (2016) used the Fourier Amplitude Sensitivity Test (FAST; Cukier, Fortuin, & Shuler, 1973; Cukier, Schaibly, & Shuler, 1975; Saltelli, Ratto, & Tarantola, 2006; Schaibly & Shuler, 1973) to identify dominant hydrologic processes (such as baseflow, evapotranspiration, run-off, infiltration, snowmelt, soil

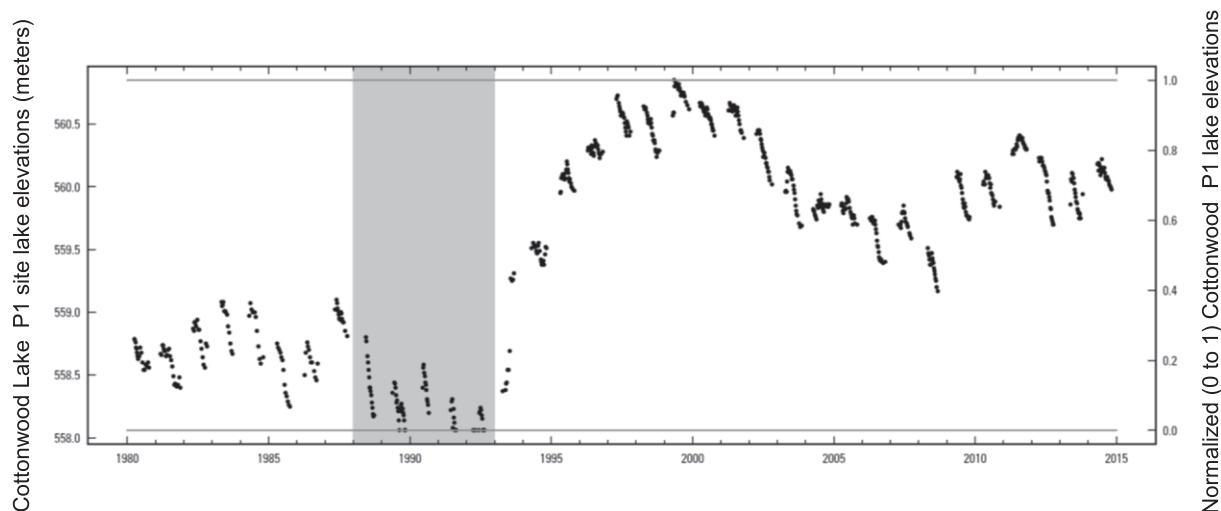


FIGURE 7 Cottonwood Lake P1 site lake elevations (black dots). Grey-shaded area indicates the 1988–92 drought period

moisture, surface run-off, and interflow) based on a CONUS-wide sensitivity analysis of PRMS parameters from the USGS NHM. Markstrom et al. (2016) found snowmelt to be the dominant process in the Upper Pipestem Creek basin; therefore, the first step in the procedure calibrated the snow accumulation and melt parameters (Table 1, green). The objective function (OF) to determine how close the simulation results are to observed values is calculated as follows:

$$OF_{\text{step1}} = \text{NRMSE}_{\text{daily}} + \text{NRMSE}_{\text{mam}} + \left(2.0 \cdot \text{NRMSE}_{\text{mthmn}}\right) + \left(2.0 \cdot \text{NRMSE}_{\text{ann}}\right) \quad (2)$$

where OF_{step1} is the sum of four OFs that calculate the normalized root mean square error (NRMSE) between observed and simulated streamflow for (a) daily values across the entire WY ($\text{NRMSE}_{\text{daily}}$); (b) daily values during March, April, and May (i.e., snowmelt season; $\text{NRMSE}_{\text{mam}}$); (c) monthly mean values ($\text{NRMSE}_{\text{mthmn}}$); and (d) annual values ($\text{NRMSE}_{\text{ann}}$). Monthly mean and annual OFs were weighted twice as much as the daily OFs due to the greater uncertainty associated with the daily streamflow observations. The weighting of the OFs was determined through trial and error.

The second and third steps in the calibration procedure calibrated the parameters that predominantly influenced high and low streamflow, respectively (Table 1, blue and red) based on a FAST parameter sensitivity analysis. The environmental flow components (EFC) algorithm developed by The Nature Conservancy (2009) was used to categorize the observed daily streamflow into high and low flow values. The EFC algorithm was coded using the default parameters for the high flow threshold (75th percentile of daily flows), low flow threshold (50th percentile of daily flows), high flow start rate threshold (25%), and high flow end rate threshold (10%). Figure 8 shows the EFC categorization results over time and the associated ranges for the five EFC components: large floods, small floods, high flow pulses, low flows, and extreme low flows. For this study, high flows consisted of flows that the EFC categorized as large floods and small floods, and high flow pulses and low flows consisted of flows that the EFC categorized as low and extreme low flows. The FAST

parameter sensitivity analysis was used to identify parameters that had the most influence on high flows (second calibration step) and low flows (third calibration step). The composite OF for the second and third calibration steps is the sum of four OFs, similar to step one, but using only high (blue, cyan, and green in Figure 8) or low (orange and red in Figure 8) daily flow values, respectively.

The fourth step in the calibration procedure calibrated the remaining parameters (Table 1, yellow) using the same OF as step one.

For the fifth step of the PRMS calibration, the FAST parameter sensitivity analysis was used to identify parameters that had the most influence on surface-water depression volume. In the five-step calibration procedure, the depression storage parameters (Table 1, grey) were removed from the preceding calibration steps and calibrated by comparing the normalized lake elevation measurements from the Cottonwood Lake P1 site (Figure 7) to the simulated PRMS variable dprst_vol_frac (fraction of the maximum storage volume of surface-water depression storage), by HRU, on a daily time step, using a NRMSE OF.

Calibration and evaluation years covered the 33-year period (WYs 1982–2014). WY 1981 was used for model initialization. Calibration and evaluation years were determined based on ranking the annual total streamflow and selecting every other ranked year for calibration or evaluation. This ensured an even distribution of dry and wet hydrologic conditions that were available for calibration and evaluation.

4 | RESULTS

The following section compares the streamflow and surface-water depression storage results from the PRMS Pipestem model using the four- and five-step calibration procedures.

4.1 | Streamflow

Figure 9 shows the observed and simulated annual streamflow from the four- (Figure 9a,b) and five-step (Figure 9a,c) calibration procedures. Figure 9a plots observed versus simulated streamflow, whereas

TABLE 1 Parameter names, ranges, descriptions, and classifications for the four- and five-step calibration procedures

Parameter				Calibration	
				Four-step	Five-step
Name	Minimum	Maximum	Description	1 Snow 2 High flows 3 Low flows 4 All flows	1 Snow 2 High flows 3 Low flows 4 All flows 5 Storage
adjmix_rain	0.6	1.4	Adjustment factor for rain in a rain/snow mix	1	1
careamax	0.1	0.9	Maximum possible percent area contributing to surface run-off	4	4
cecn_coef	4.0	6.0	Monthly convection condensation energy coefficient	2	2
dprst_depth_avg	20.0	300.0	Average depth of storage depressions at maximum storage capacity	3	5
dprst_et_coef	0.0	1.0	Fraction of unsatisfied potential evapotranspiration (PET) applied to surface depression storage	3	5
dprst_flow_coef	0.0001	0.1	Coefficient in linear flow routing equation for open surface depressions	2	5
dprst_seep_rate_open	0.00001	0.1	Coefficient used in linear seepage flow equation for open surface depressions	3	5
emis_noppt	0.757	1	Average emissivity of air on days without precipitation	1	1
fastcoef_lin	0.01	0.4	Linear coefficient in equation to route preferential-flow storage down slope	3	3
fastcoef_sq	0.00001	0.8	Nonlinear preferential-flow routing coefficient	2	2
freeh2o_cap	0.01	0.1	Free-water holding capacity of snowpack	1	1
gwflow_coef	0.02	0.06	Linear coefficient in the equation to compute groundwater (gw) discharge	3	3
op_flow_thres	0.75	1.0	Fraction of open depression storage above which surface run-off occurs	2	5
potet_sublim ¹	0.4	0.6	Fraction of PET that is sublimated from snow in the canopy and snowpack	1	1
pref_flow_den	0.0	0.09	Fraction of the soil zone in which preferential flow occurs	4	4
rad_trncf	0.015	1.0	Transmission coefficient for short-wave radiation through winter vegetation canopy	1	1
radmax	0.5	0.9	Maximum fraction of the potential solar radiation that may reach the ground	1	1
rain_cbh_adj	0.5	3	Monthly adjustment factor to measured precipitation	4	4
sat_threshold	0.0001	200.0	Soil saturation threshold, above field-capacity threshold	2	5
slowcoef_lin	0.00001	0.5	Linear gravity-flow reservoir routing coefficient	2	2
slowcoef_sq	0.05	0.35	Nonlinear coefficient in equation to route gravity-reservoir storage down slope	3	3
smidx_coef	0.0	0.06	Coefficient in nonlinear contributing area algorithm	2	2
smidx_exp	0.0001	1.0	Exponent in nonlinear contributing area algorithm	4	4
snow_intcp	0.01	0.95	Snow interception storage capacity	1	1
snowinfil_max	0.0	20.0	Maximum snow infiltration	1	1
snow_cbh_adj	0.5	3.0	Monthly adjustment factor to measured precipitation	1	1
soil2gw_max	0.0	0.35	Maximum amount of capillary reservoir excess routed directly to gw reservoir	2	2
soil_moist_max	1.0	10.0	Maximum available water holding capacity of capillary reservoir	3	3
soil_rechr_max_frac	0.02	1.0	Maximum storage for soil recharge zone as fraction of soil_moist_max	2	2
srain_intcp	0.01	0.95	Summer rain interception storage capacity for the major vegetation type	3	3
ssr2gw_exp	0.0	3.0	Coefficient to route water from subsurface to groundwater	4	4
ssr2gw_rate	0.01	0.8	Coefficient to route water from gravity reservoir to gw reservoir	2	2
tmax_allrain_offset	0.1	9.5	Added to tmax_allsnow; temperature when precipitation is assumed to be rain	1	1
tmax_allsnow	29.0	40.0	Monthly maximum air temperature when precipitation is assumed to be snow	1	1
tmax_cbh_adj	-3	3	Monthly maximum air temperature adjustment factor	4	4
tmin_cbh_adj	-3	3	Monthly minimum air temperature adjustment factor	4	4
wrain_intcp	0.01	0.95	Winter rain interception storage capacity	3	3

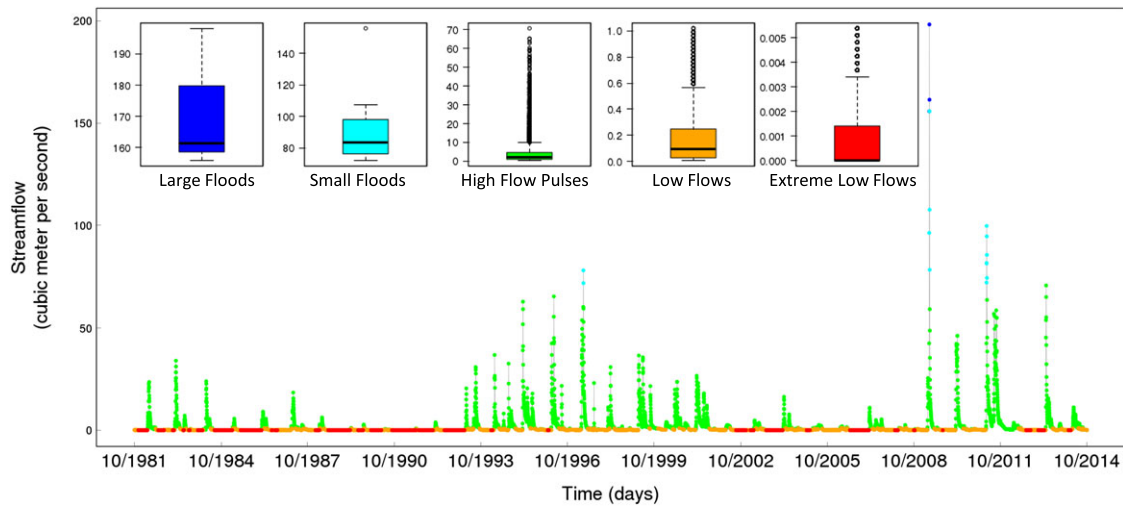


FIGURE 8 Environmental flow components for daily observed streamflow at U.S. Geological Survey streamgage 06469400 (Pipestem Creek near Pingree, North Dakota): large floods (blue), small floods (cyan), high flow pulses (green), low flows (orange), and extreme low flows (red)

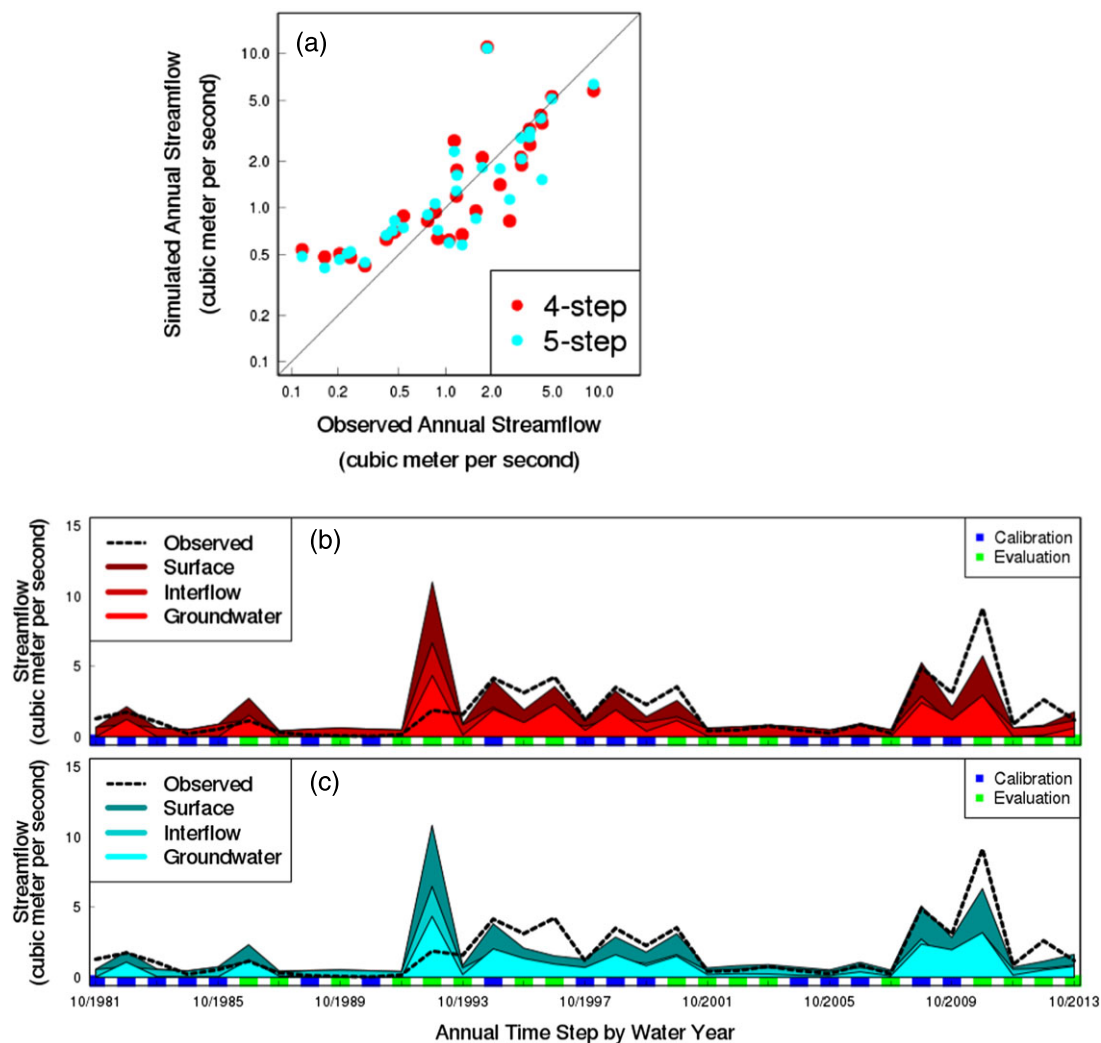


FIGURE 9 Annual observed and simulated mean streamflow using the four- and five-step calibration procedures: (a) observed versus simulated (diagonal line shows the 1:1 relation) and (b) observed and simulated (four-step) over time and (c) observed and simulated (five-step) over time. Blue indicates calibration years, and green indicates evaluation years

Figure 9b (four-step calibration) and 9c (five-step calibration) compare observed streamflow to the simulated model components of annual flow (surface run-off, interflow, and groundwater flow; Figure 5). The calibration (blue) and evaluation (green) years are indicated along the lower x axis of Figure 9b,c. Table 2 lists the NRMSE for the calibration and evaluation periods from the four- and five-step calibration procedures. On an annual time step, there is very little difference in the simulated streamflow results between the calibration procedures. The evaluation period shows a decrease in annual accuracy compared to the calibration period for both calibrations (Table 2).

Figure 10 shows the observed and simulated monthly mean streamflow results from the four- and five-step calibration procedures. Because of the log scale in Figure 10a, observed monthly values less than $0.0001 \text{ m}^3/\text{s}$ (approximately 10% of the record) are not shown. Figure 10a illustrates the tendency of the simulations to overestimate the very low flow values. Figure 10b indicates that the accuracy of the simulated monthly mean streamflow is highly variable. On a monthly time step, there is little difference in simulated streamflow between

the calibration procedures. The evaluation period shows a decrease in monthly accuracy compared to the calibration period (Table 2).

Figure 11a compares observed and simulated daily mean streamflow using the four- and five-step calibration procedures, further emphasizing the model tendency to overestimate the very low flow values. Table 2 lists the NRMSE for the calibration and evaluation periods using the four- and five-step calibration procedures. On a daily time step, there is a slight increase in accuracy from the four- to the five-step procedure. The evaluation period shows a decrease in daily accuracy over the calibration period (Table 2). Figure 11b–d compares the simulated model components of flow (surface run-off, interflow, and groundwater flow) produced using the four- and five-step calibration procedures. Simulations of surface run-off and interflow are largely similar between the two calibration scenarios (Figure 11b,c). Simulations of low groundwater flows are generally larger for the five-step calibration scenario that includes information about lake levels in the optimization procedure (Figure 11d). In addition, for mid-range groundwater flows, the five-step does not vary as much as the four-step-based flows, indicating that the surface depression storage is buffering the hydrologic response during those conditions.

TABLE 2 Normalized root mean square error between observed and simulated run-off

Time step	Normalized root mean square error			
	Calibration period		Evaluation period	
	Four-step	Five-step	Four-step	Five-step
Annual	0.0214	0.0221	0.1280	0.1268
Monthly	0.0501	0.0533	0.1865	0.1934
Daily	0.0938	0.0759	0.2742	0.2697

4.2 | Surface-water depression storage

Figure 12a,b compare the observed normalized Cottonwood Lake P1 site lake elevations and the fractional surface depression storage for each HRU on a daily time step for the four- and five-step calibration procedures, respectively. The four-step procedure did not reproduce depression storage that resulted in any volume that would approach

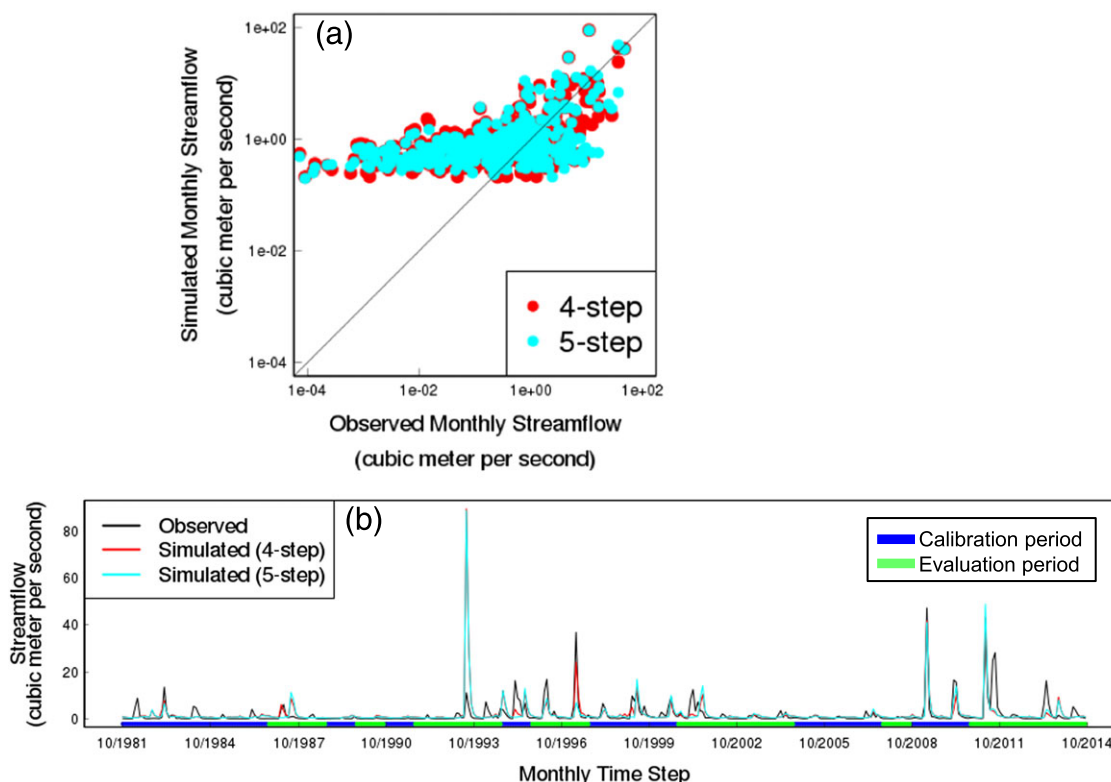


FIGURE 10 Monthly observed and simulated mean streamflow using the four- and five-step calibration procedures: (a) observed versus simulated (diagonal line shows the 1:1 relation) and (b) observed and simulated over time. Blue lines indicate calibration years, and green lines indicate evaluation years

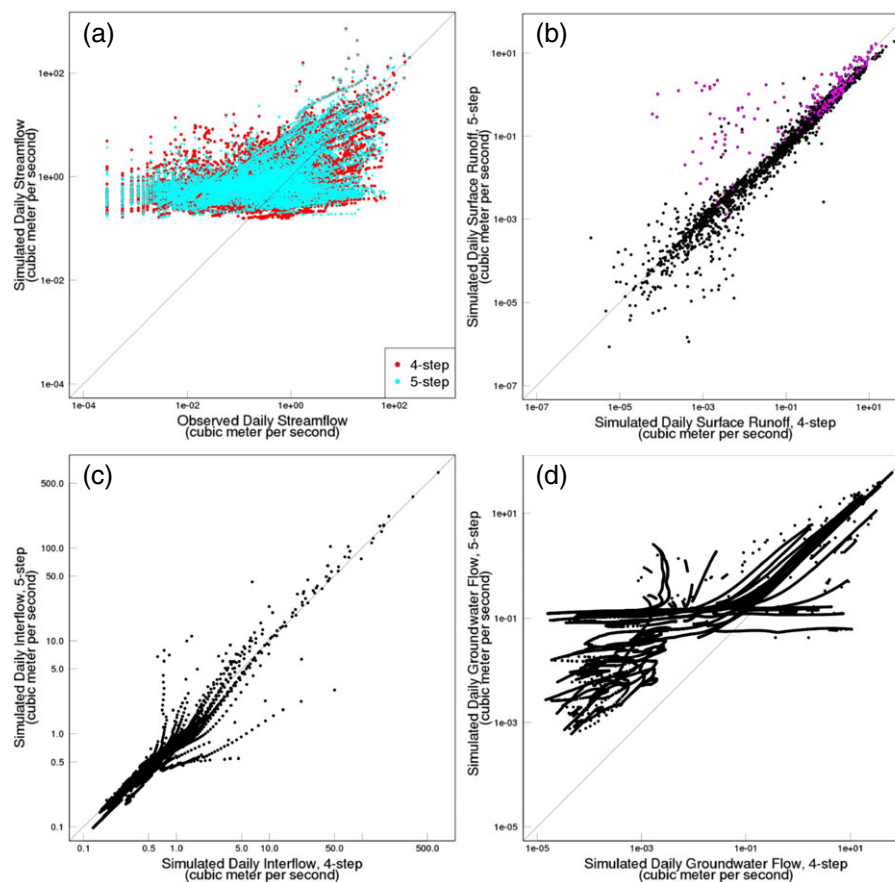


FIGURE 11 Daily mean streamflow: (a) observed versus simulated and four- versus five-step calibration procedure: (b) surface runoff, (c) interflow, and (d) groundwater flow. Magenta dots in (b) correspond to spillage events in Figure 13a. Diagonal lines show the 1:1 relation

spill levels for any HRU (coloured lines in Figure 12a), indicating that there was not enough information in the streamflow data to calibrate the depression storage parameters. The five-step procedure was able to match the HRU fractional storage to the observed normalized Cottonwood Lake P1 site lake elevations for all HRUs with depression storage (Figure 12b), resulting in surface depression runoff when the HRU depression storage was exceeded.

Including depression storage in the model calibration (five-step) has the effect of increasing the smallest groundwater values (Figure 11d). Conceptually, this makes sense; depression storage seep contributes to groundwater recharge (Figure 6c), and the four-step procedure maintained relatively little water volume in the surface depression storages (Figure 12a).

Figure 13a shows the surface depression runoff (or spillage) that occurred when filling of the aggregated-surface depressions resulted in spilling to runoff in the five-step calibration procedure. These events correspond to the higher five-step surface runoff values highlighted in magenta in Figure 11b. Figure 13b shows the probability of surface depression spillage by month, with no spilling during the colder months when water in the depressions is most likely frozen.

5 | DISCUSSION

The PRMS model was tested with two calibration procedures: (a) a four-step methodology that calibrated parameters to a water balance

and components of the daily hydrograph and (b) a five-step methodology that calibrated parameters to a water balance, components of the daily hydrograph, and the normalized lake elevations from the Cottonwood Lake P1 site. As noted earlier, the observed streamflow data accuracy was considered fair to poor, with a substantial portion of the observed streamflow record with zero, or close to zero, streamflow (Figure 4). These zero flow days typically occur in late summer when the stream network becomes disconnected (written comm., Renee Brooks, February 2017). The streamflow simulation results from both calibration procedures were not highly accurate for many years, but problems with simulating streamflow in the cold, semiarid climate are not uncommon (Bock et al., 2016; Martinez & Gupta, 2010; Newman et al., 2015). Although both calibration procedures produced comparable simulated streamflow results, only the five-step methodology produced realistic changes in surface-water depression storage, indicating that in the PPR, a proxy for surface-water depression storage change is needed to accurately parameterize surface-water depression storage.

The four-step methodology, while producing simulated streamflow similar to the five-step, incorrectly portrayed the changes in surface-water depression storage; in effect, the four-step produced the “right” answer (e.g., streamflow) for the “wrong” reasons (e.g., unrealistic surface-water depression storage representation). This underscores the importance of understanding the local characteristics of the modelling area under consideration. The net effect of the five-step calibration procedure was not improved simulation of streamflow but

Normalized Cottonwood Lake P1 Site Lake Elevations and HRU Fractional Storage

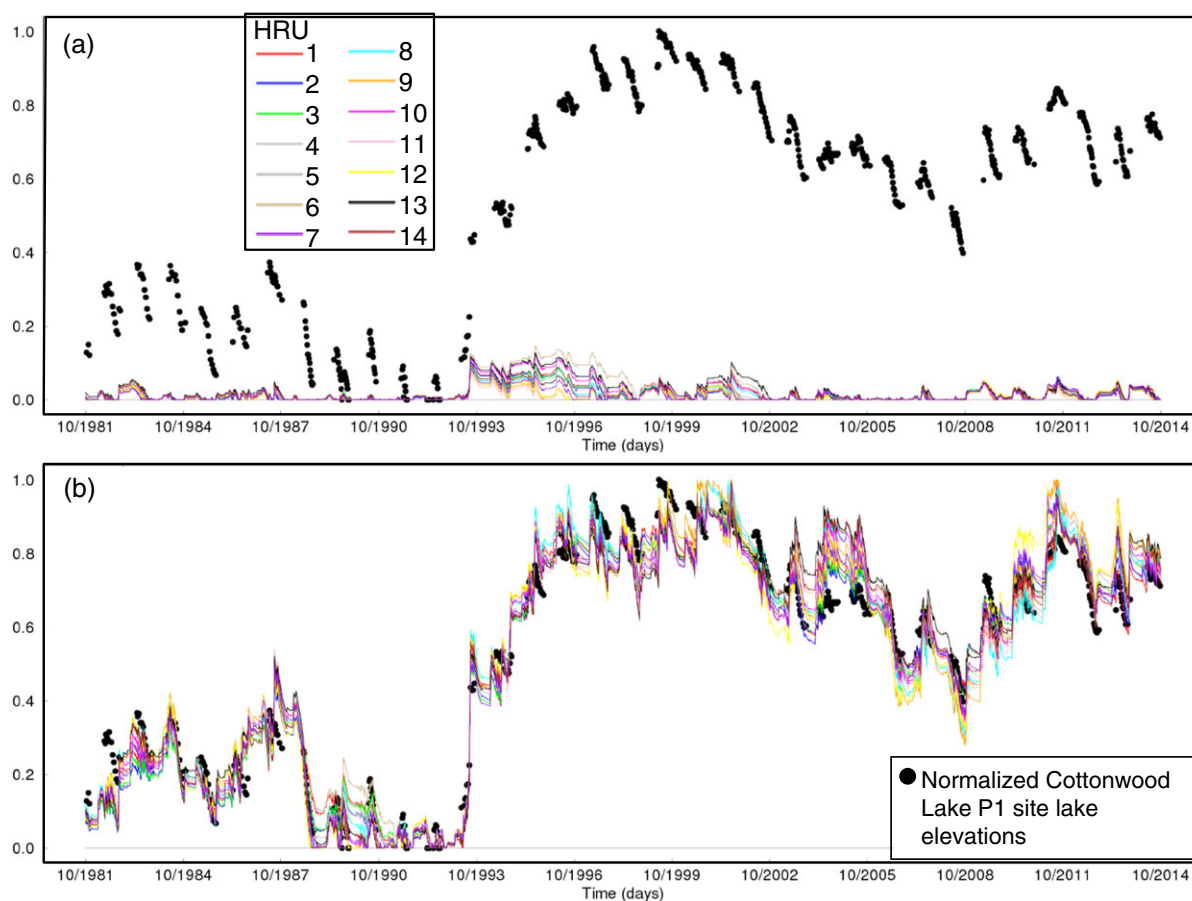


FIGURE 12 Normalized Cottonwood Lake P1 site lake elevations and hydrologic response unit (HRU) fractional storage for the (a) four-step and (b) 5-step calibration procedures

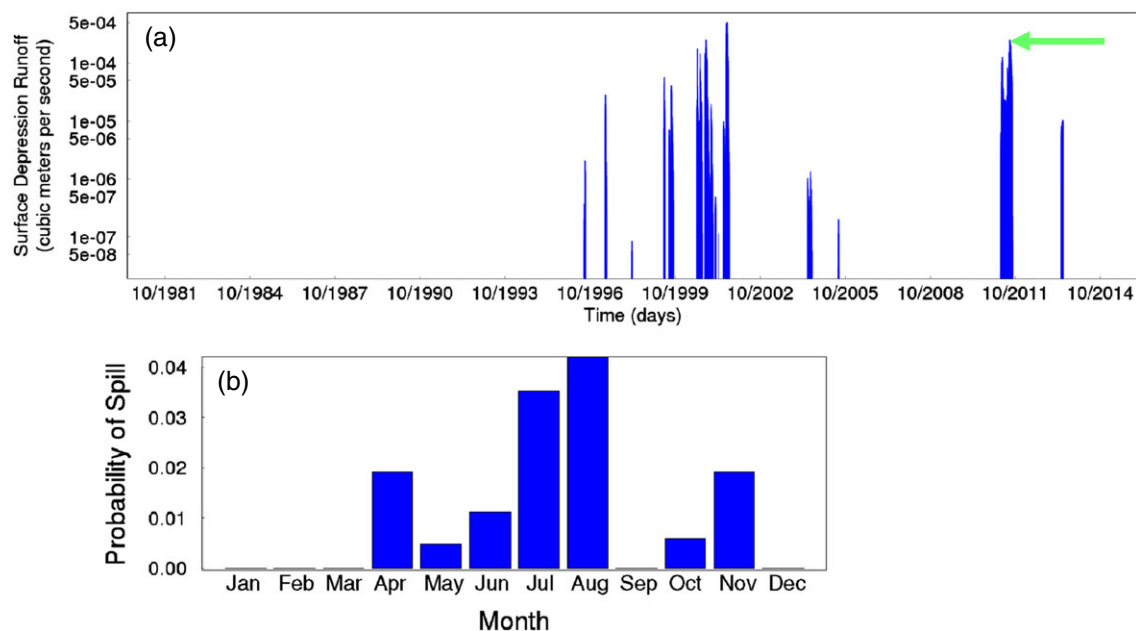


FIGURE 13 Five-step calibration results: (a) surface-water depression runoff and (b) probability of surface-water depression spillage by month. The green arrow designates the highest value for the remotely sensed surface-water depression areas

rather more accurate representation of surface-water depression storage in the water balance (a critical habitat for many aquatic species; Colburn, 2004) and perhaps a more accurate representation of the relative distribution of the components of streamflow.

To demonstrate this last point, Figure 14 shows the relative contribution to total streamflow from the components of streamflow (groundwater flow, interflow, and surface runoff) by month using the five- and four-step calibration procedure. Note that contributions from surface-water depression storage seepage and spillage are minimal in the overall water balance. The components of streamflow are distributed differently between the two calibration procedures. In general, surface runoff is reduced, and groundwater flow is increased in the five- versus four-step calibration results—a direct result of surface-water depressions capturing the surface runoff and seepage to groundwater (Figure 5b). There are other processes that depend on effectively modelling the components of flow. For example, PRMS contains a stream temperature module (Sanders, Markstrom, Regan, & Atkinson, 2017) that produces daily mean and maximum water temperatures at the outflow of each stream segment defined in a PRMS model. Temperatures are associated with the fluxes of each

component of streamflow. If these are not accurately represented, then stream temperatures will be misrepresented.

A challenge with larger-scale streamflow models, such as the NHM, is finding datasets and products that can be used to calibrate model processes. Improved representation of processes using global gridded products can result in more accurate simulation of the components of streamflow for these large scale models applied in almost any location. Some of the currently available global products include surface-water extent (Pekel, Cottam, Gorelick, & Belward, 2016), inundation extent (Aires et al., 2017), snow (Frei et al., 2012; Riggs & Hall, 2016), and evapotranspiration (Zhang, Kimball, Nemani, & Running, 2010). Small-scale studies can apply local knowledge to modelling areas that can provide further refinement and improvement to large-scale models.

This modelling study in the PPR provided valuable insight into the type of ancillary information that could be used to calibrate surface-water depression storage. For this study, the proxy for change in surface-water depression storage was normalized lake elevations from the Cottonwood Lake P1 site in the nearby Cottonwood Lake study area; an example of using local knowledge to improve understanding

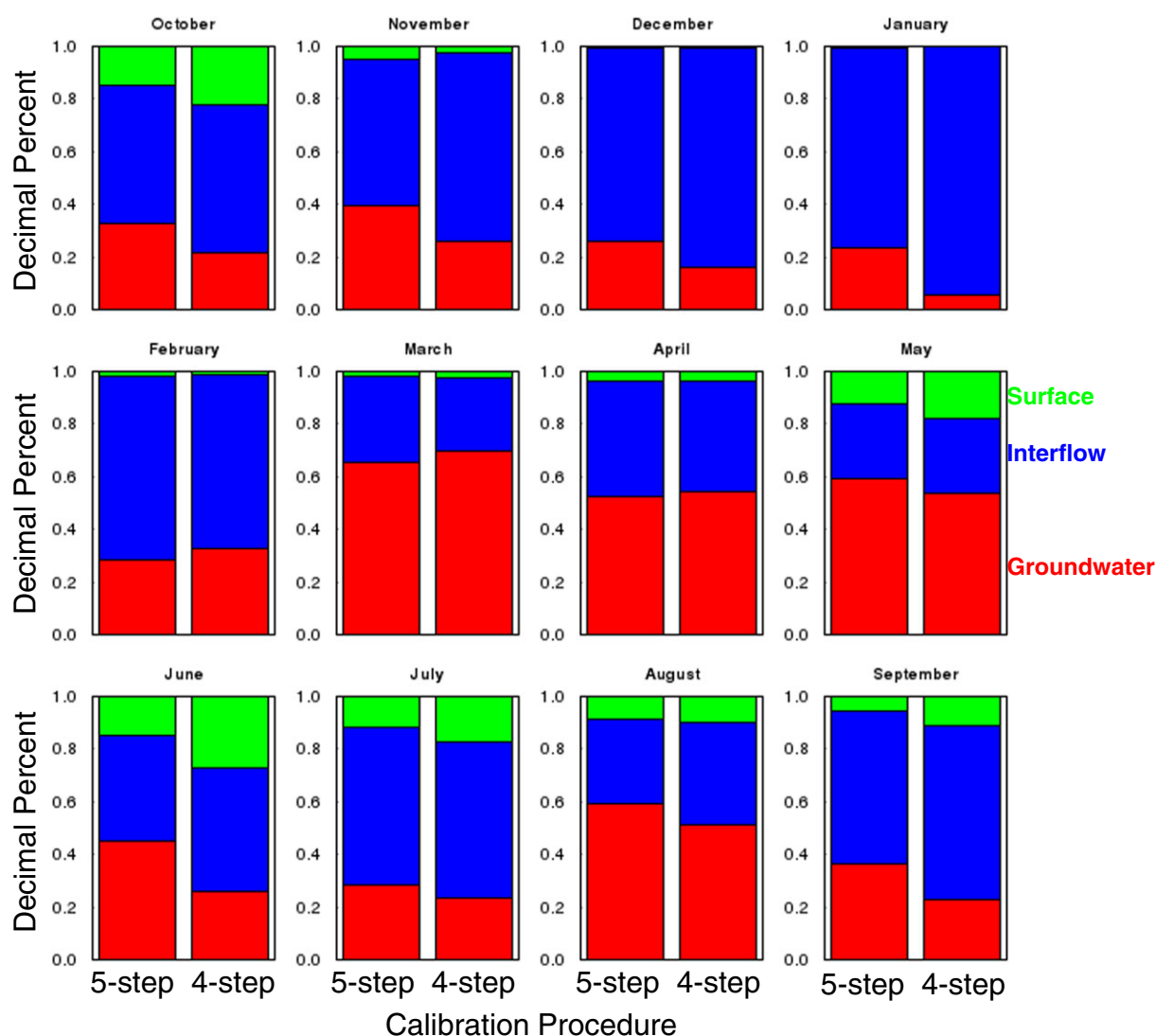


FIGURE 14 Per cent contribution to total streamflow by month using the five- and four-step calibration procedure: groundwater flow (red), interflow (blue), and surface run-off (green)

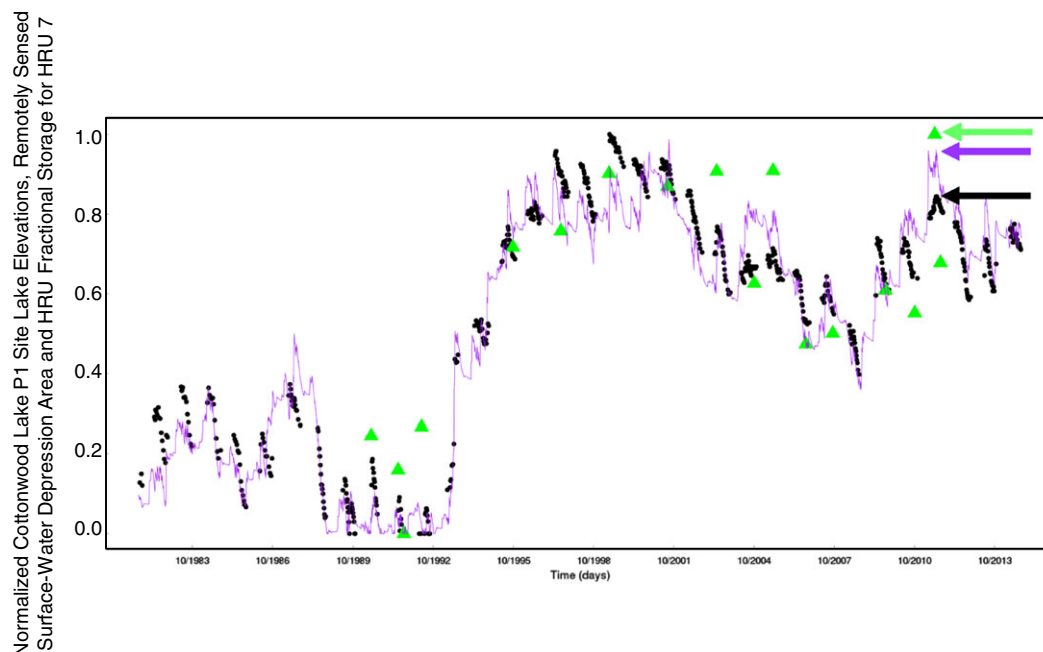


FIGURE 15 Normalized Cottonwood Lake P1 site lake elevations (black dots), remotely sensed surface-water depression areas for hydrologic response unit (HRU) 7 (green triangles), and fractional storage for HRU 7 (purple line). The green arrow designates the highest value for the remotely sensed surface-water depression areas with purple and black arrows designating the corresponding simulated and observed values, respectively

and representation of processes at local scale within the larger CONUS model. Many study areas may not have useful nearby proxies like the Upper Pipestem Creek basin; however, other data sources could potentially be used to indicate changes in surface-water depression storage that may also allow for the calibration of surface-water depression storage at larger spatial scales, including that of the CONUS. For example, surface-water extent derived from remotely sensed imagery could be used to estimate changes in surface-water depression storage. By relating surface-water extent to datasets such as NHDPlus, the fraction of stream-connected and nonstream connected surface-water extent can be estimated (Vanderhoof et al., 2015). In Figure 15, the normalized Cottonwood Lake P1 site lake elevations (black dots) are plotted along with normalized surface depression areas as mapped from Landsat imagery (Vanderhoof et al., 2015; green triangles) for HRU 7 (largest HRU in the Upper Pipestem Creek basin, see Figures 1 and 2) and PRMS-simulated fractional storage for HRU 7 (purple line). Compiling this remotely sensed information for the CONUS would improve parameterization of the USGS surface-water depression storage algorithm for the CONUS, and this same type of analysis could potentially be applied to other models worldwide. The USGS is currently working to generate a Dynamic Surface-Water Extent product using the Landsat archive (1984–present) that would provide data on surface-water temporal variability at 30-m spatial resolution across the CONUS (Jones, 2015).

The highest value for the remotely sensed surface depression areas (green arrow in Figure 15) corresponds to the largest surface depression runoff events in 2011 (green arrow in Figure 13a). Note that the normalized Cottonwood Lake P1 site lake elevations were closer to 85% of their maximum recorded values at that time (black arrow in Figure 15), but the PRMS five-step calibration resulted in HRU 7 fractional surface-water depression storage higher than the

normalized Cottonwood Lake elevations (purple arrow, Figure 15). This inconsistency may be the product of using water level measurements from a single, small pond feature. Topography adjacent to a depression has been shown to influence how changes in water level translate to changes in surface-water extent or spillage (Rover, Wright, Euliss, Mushet, & Wylie, 2011), implying that a change in water level cannot be expected to produce consistent changes in connections across the landscape. In addition, temporary wetland-stream connections in the PPR have been shown to occur disproportionately in particularly wet years (Vanderhoof et al., 2015), implying that the importance of including a temporally variable depression storage estimate may be less important in drier years but particularly important in wet years.

6 | SUMMARY AND CONCLUSIONS

The PRMS was used to simulate changes in surface-water depression storage in the 1,126-km² Upper Pipestem Creek basin located within the PPR of North Dakota. The Upper Pipestem PRMS model consists of 14 HRUs extracted from the USGS's NHM. Each HRU in the USGS NHM was parameterized using aggregated surface-water depression area. A calibration dataset for surface depression storage was developed for this study based on normalized lake elevations from the Cottonwood Lake P1 site in the Cottonwood Lake study area, a long-term wetland ecosystem monitoring site located just south of the Upper Pipestem Creek basin. Two calibration procedures were tested: (a) a four-step methodology that calibrated parameters to a water balance and components of the daily hydrograph and (b) a five-step methodology that calibrated parameters to a water balance, components of the daily hydrograph, and normalized Cottonwood Lake P1 site lake elevations. Results indicate that simulated streamflow was similar

for both calibration strategies but only the five-step methodology produced realistic changes in surface-water depression storage. This study indicates that a regionalized parameterization of the USGS NHM will require a proxy for change in surface storage to accurately parameterize surface-water depression storage for the CONUS.

ORCID

Lauren Hay  <http://orcid.org/0000-0003-3763-4595>

Roland Viger  <http://orcid.org/0000-0003-2520-714X>

REFERENCES

- Aires, F., Miolane, L., Prigent, C., Pham, B., Fluet-Chouinard, E., Lehner, B., & Papa, F. (2017). A global dynamic and long-term inundation extent dataset at high spatial resolution derived through downscaling of satellite observations. *Journal of Hydrometeorology*, 18, 1305–1325. <https://doi.org/10.1175/JHM-D-16-0155.1>
- Barton, A. B., Herczeg, A. L., Dahlhaus, P. G., & Cox, J. W. (2013). A geochemical approach to determining the hydrological regime of wetlands in a volcanic plain, south-eastern Australia. In L. Ribeiro, T. Y. Stigter, A. Chambel, M. T. de Melo Condesso, J. P. Monteiro, & A. Medeiros (Eds.), *Groundwater and ecosystems*. Boca Raton: CRC Press.
- Blodgett, D. L., Booth, N. L., Kunicki, T. C., Walker, J. I., & Viger, R. J. (2011). Description and testing of the geo data portal: A data integration framework and web processing services for environmental science collaboration, U.S. Geological Survey Open-File Report 2011–1157, 9 pp. [Also available at <https://pubs.er.usgs.gov/publication/ofr20111157>.]
- Bock, A. R., Hay, L. E., McCabe, G. J., Markstrom, S. L., & Atkinson, R. D. (2016). Parameter regionalization of a monthly water balance model for the conterminous United States. *Hydrology and Earth System Sciences*, 20, 2861–2876. <https://doi.org/10.5194/hess-20-2861-2016>
- Campo, L., Caparrini, F., & Castelli, F. (2006). Use of multi-platform, multi-temporal remote-sensing data for calibration of a distributed hydrological model: An application in the Arno basin, Italy. *Hydrological Processes*, 20, 2693–2712. <https://doi.org/10.1002/hyp.6061>
- Cao, W., Sun, Ge, McNulty, S. G., Chen, J., Noormets, A., Skaggs, R. W., & Amatya, D. M. (2006). Evapotranspiration of a mid-rotation loblolly pine plantation and a recently harvested stands on the coastal plain of North Carolina, U.S.A. In Williams, Thomas, eds., *Hydrology and Management of Forested Wetlands: Proceedings of the International Conference, St. Joseph, MI, American Society of Agricultural and Biological Engineers*, pp. 27–33. Retrieved from <https://www.treesearch.fs.fed.us/pubs/22421> [Accessed January 30, 2017].
- Cohen, M. J., Creed, I. F., Alexander, L., Basu, N. B., Calhoun, A. J. K., Craft, C., ... Walls, S. C. (2016). Do geographically isolated wetlands influence landscape functions? *PNAS*, 113(8), 1978–1986. <https://doi.org/10.1073/pnas.1512650113> [Accessed January 30, 2017].
- Colburn, E. A. (2004). *Vernal pools—Natural history and conservation*. Blacksburg, VA: The McDonald & Woodward Publishing Company.
- Cukier, R. I., Fortuin, C. M., & Shuler, K. E. (1973). Study of the sensitivity of coupled reaction systems to uncertainties in rate coefficients. I *Theory*, *Journal of Chemical Physics*, 59(8), 3873–3878.
- Cukier, R. I., Schaibly, J. H., & Shuler, K. E. (1975). Study of the sensitivity of coupled reaction systems to uncertainties in rate coefficients. III *The Journal of Chemical Physics*, 63(3), 1140–1149.
- De Laney, T. A. (1995). Benefits to downstream flood attenuation and water quality as a result of constructed wetlands in agricultural landscapes. *Journal of Soil and Water Conservation*, 50(6), 620–626. Retrieved from <http://www.jswnonline.org/content/50/6/620.extract>
- Driscoll, J. M., Markstrom, S. L., Regan, R. S., Hay, L. E., & Viger, R. J. (2017). National Hydrologic Model Parameter Database: 2017-05-08 download. U.S. Geological Survey. <https://doi.org/10.5066/F7NS0SCW>
- Duan, Q., Sorooshian, S., & Gupta, V. (1992). Effective and efficient global optimization for conceptual rainfall-runoff models. *Water Resources Research*, 28(4), 1015–1031. <https://doi.org/10.1029/91WR02985> [Accessed February 9, 2017].
- Duan, Q., Sorooshian, S., & Gupta, V. K. (1994). Optimal use of the SCE-UA global optimization method for calibrating watershed models. *Journal of Hydrology*, 158(3–4), 265–284. [https://doi.org/10.1016/0022-1694\(94\)90057-4](https://doi.org/10.1016/0022-1694(94)90057-4) [Accessed February 9, 2017].
- Duan, Q. Y., Gupta, V. K., & Sorooshian, S. (1993). Shuffled complex evolution approach for effective and efficient global minimization. *Journal of Optimization Theory and Applications*, 76(3), 501–521. <https://doi.org/10.1007/BF00939380>
- Eisenlohr, W. S., & Sloan, C. E. (1968). Generalized hydrology of prairie pot-holes on the Coteau du Missouri, North Dakota: U.S. Geological Survey Circular 558. Retrieved from <https://pubs.er.usgs.gov/publication/cir558> [Accessed February 9, 2017].
- Evenson, G. R., Golden, H. E., Lane, C. R., & D'Amico, E. (2016). An improved representation of geographically isolated wetlands in a watershed-scale hydrologic model. *Hydrological Processes*, 30, 4168–4184. <https://doi.org/10.1002/hyp.10930> [Accessed February 9, 2017].
- Flint, R. F. (1971). *Glacial and quaternary geology*. (pp. 892). New York: John Wiley and Sons.
- Franz, K. J., & Karsten, L. R. (2013). Calibration of a distributed snow model using MODIS snow covered area data. *Journal of Hydrology*, 494, 160–175. <https://doi.org/10.1016/j.jhydrol.2013.04.026> [Accessed January 27, 2017].
- Frei, A., Tedesco, M., Lee, S., Foster, J., Hall, D. K., Kelly, R., & Robinson, D. A. (2012). A review of global satellite-derived snow products. *Advances in Space Research*, 50(8), 1007–1029 ISSN 0273-1177. <https://doi.org/10.1016/j.asr.2011.12.021>
- Golden, H. E., Lane, C. R., Amatya, D. M., Bandilla, K. W., Raanan Kiperwas, H., Knightes, C. D., & Ssegane, H. (2014). Hydrologic connectivity between geographically isolated wetlands and surface water systems: A review of select modeling methods. *Environmental Modelling & Software*, 53, 190–206. <https://doi.org/10.1016/j.envsoft.2013.12.004> [Accessed February 9, 2017].
- Hay, L. E., Leavesley, G. H., & Clark, M. P. (2006) Use of remotely-sensed snow covered area in watershed model calibration for the Sprague River, Oregon. Joint 8th Federal Interagency Sedimentation Conference and 3rd Federal Interagency Hydrologic Modeling Conference, April 2–6, 2006, Reno, Nevada.
- Hay, L. E., Leavesley, G. H., Clark, M. P., Markstrom, S. L., Viger, R. J., & Umemoto, M. (2006). Step wise multiple objective calibration of a hydrologic model for a snowmelt dominated basin. *Journal of the American Water Resources Association*, 42(4), 877–890. <https://doi.org/10.1111/j.1752-1688.2006.tb04501.x>
- Hay, L. E., & Umemoto, M. (2007). *Multiple-objective stepwise calibration using Luca*. U.S. Geological Survey Open-File Report 2006–1323, 25p. <https://pubs.er.usgs.gov/publication/ofr20061323>
- Homer, C., Dewitz, J., Fry, J., Coan, M., Hossain, N., Larson, C., ... Wickham, J. (2007). Completion of the 2001 National Land Cover Database for the conterminous United States. *Photogrammetric Engineering and Remote Sensing*, 73(4), 337–341.
- Huang, S., Dahal, D., Young, C., Chander, G., & Liu, S. (2011). Integration of Palmer Drought Severity Index and remote sensing data to simulate wetland water surface from 1910 to 2009 in Cottonwood Lake area, North Dakota. *Remote Sensing of Environment*, (12), 115, 3377–3389. <https://doi.org/10.1016/j.rse.2011.08.002> [Accessed January 27, 2017].
- Immerzeel, W. W., & Droogers, P. (2008). Calibration of a distributed hydrological model based on satellite evapotranspiration. *Journal of Hydrology*, 349(3–4), 411–424. <https://doi.org/10.1016/j.jhydrol.2007.11.017> [Accessed January 30, 2017].
- Ilsenstein, E. M., Wi, S., & Yang, Y. C. E. (2015). Calibration of a distributed hydrologic model using streamflow and remote sensing snow data. World environmental and water resources congress 2015: Floods, droughts, and ecosystems. ASCE, 973–982. <https://doi.org/10.1061/9780784479162.093#sthash.4tY0fBA1.dpuf>

- Jones, J. W. (2015). Efficient wetland surface water detection and monitoring via Landsat: Comparison with in situ data from the Everglades depth estimation network. *Remote Sensing*, 7(9), 12503–12538.
- Kennedy, E. J. (1983) Computation of continuous records of streamflow, U. S. Geological Survey Techniques of Water-Resources Investigations, book 3, chap. A13, 53 p. Retrieved from <https://pubs.er.usgs.gov/publication/twri03A13> [Accessed January 25, 2017].
- Koren, V., Morel, F., & Smith, M. (2008). Use of soil moisture observations to improve parameter consistency in watershed calibration. *Physics and Chemistry of the Earth*, 33(17–18), 1068–1080. <https://doi.org/10.1016/j.pce.2008.01.003> [Accessed January 27, 2017].
- LaFontaine, J. H., Hay, L. E., Viger, R. J., Regan, R. S., & Markstrom, S. L. (2015). Effects of climate and land cover on hydrology in the Southeastern U.S.: Potential impacts on watershed planning. *Journal of the American Water Resources Association (JAWRA)*, 51(5), 1235–1261. <https://doi.org/10.1111/1752-1688.12304> [Accessed February 9, 2017].
- Leibowitz, S. G., Mushet, D. M., & Newton, W. E. (2016). Intermittent surface water connectivity: Fill and spill vs. fill and merge dynamics. *Wetlands*, 36(suppl. 2), 323–342.
- Leibowitz, S. G., & Vining, K. C. (2003). Temporal connectivity in a prairie pothole complex. *Wetlands*, 23(1), 13–25. [https://doi.org/10.1672/0277-5212\(2003\)023%5B0013:TCIAPP%5D2.0.CO;2](https://doi.org/10.1672/0277-5212(2003)023%5B0013:TCIAPP%5D2.0.CO;2) [Accessed January 27, 2017].
- Ludden, A. P., Frink, D. L., & Johnson, D. H. (1983). Water storage capacity of natural wetland depressions in the Devils Lake Basin of North Dakota. *Journal of Soil and Water Conservation*, 38(1), 45–48.
- Markstrom, S. L., Hay, L. E., & Clark, M. P. (2016). Towards simplification of hydrologic modeling: Identification of dominant processes. *Hydrology and Earth System Sciences*, 20, 4655–4671. <https://doi.org/10.5194/hess-20-4655-2016> [Accessed February 9, 2017].
- Markstrom, S. L., Regan, R. S., Hay, L. E., Viger, R. J., Webb, R. M. T., Payn, R. A., & LaFontaine, J. H. (2015) PRMS-IV, the precipitation-runoff modeling system, version 4, U.S. Geological Survey Techniques and Methods, book 6, chap. B7, 158 p. <https://doi.org/10.3133/tm6B7>.
- Martinez, G. F., & Gupta, H. V. (2010). Toward improved identification of hydrologic models: A diagnostic evaluation of the “abcd” monthly water balance model for the conterminous United States. *Water Resources Research*, 46, W08507. <https://doi.org/10.1029/2009WR008294> [Accessed February 9, 2017].
- Menne, M. J., Imke, D., Vose, R. S., Gleason, B. E., & Houston, T. G. (2012). An overview of the global historical climatology network-daily database. *Journal of Atmospheric and Oceanic Technology*, 29(7), 897–910.
- Mushet, D. M., Calhoun, A. J. K., Alexander, L. C., Cohen, M. J., DeKeyser, E. S., Fowler, L., ... Walls, S. C. (2015). Geographically isolated wetlands: Rethinking a misnomer. *Wetlands*, 35(3), 423–431. <https://doi.org/10.1007/s13157-015-0631-9> [Accessed January 27, 2017].
- Mushet, D. M., & Euliss, N. H. Jr. (2012) The Cottonwood Lake study area, a long-term wetland ecosystem monitoring site, U.S. Geological Survey Fact Sheet 2012–3040, 2 p. Retrieved from <https://pubs.er.usgs.gov/publication/fs20123040> [Accessed February 9, 2017].
- Mushet, D. M., Rosenberry, D. O., Euliss Jr., N. H., & Solensky, M. J. (2016) Cottonwood Lake study area—Water surface elevations, U.S. Geological Survey data release. Retrieved from <https://doi.org/10.5066/F7707ZJ6> [Accessed February 2, 2017].
- Newman, A. J., Clark, M. P., Sampson, K., Wood, A., Hay, L. E., Bock, A., ... Duan, Q. (2015). Development of a large-sample watershed-scale hydrometeorological data set for the contiguous USA: Data set characteristics and assessment of regional variability in hydrologic model performance. *Hydrology and Earth System Sciences*, 19, 209–223. <https://doi.org/10.5194/hess-19-209-2015> [Accessed February 9, 2017].
- Parkhurst, R. S., Sturrock, A. M., Rosenberry, D. O., & Winter, T. C. (1995) Climatic and lake temperature data for Wetland P1, Cottonwood Lake Area, Stutsman county, North Dakota, 1982–87, U.S. Geological Survey Open-File Report 94–546, 40 p. Retrieved from <https://pubs.usgs.gov/of/1994/0546/report.pdf>
- Pekel, J.-F., Cottam, A., Gorelick, N., & Belward, A. S. (2016). High-resolution mapping of global surface water and its long-term changes. *Nature*, 540, 418–422. <https://doi.org/10.1038/nature20584>
- Philips, R. W., Spence, C., & Pomeroy, J. W. (2011). Connectivity and runoff dynamics in heterogeneous basins. *Hydrological Processes*, 25, 3061–3075 <https://doi.org/10.1002/hyp.8123> [Accessed January 27, 2017].
- Refsgaard, J. C. (1997). Parameterization, calibration and validation of distributed hydrological models. *Journal of Hydrology*, 198, 69–97 [https://doi.org/10.1016/S0022-1694\(96\)03329-X](https://doi.org/10.1016/S0022-1694(96)03329-X) [Accessed February 9, 2017].
- Regan, R. S., & LaFontaine, J. H. (2017) Documentation of the dynamic parameter, water-use, stream and lake flow routing, and two summary output modules and updates to surface-depression storage simulation and initial conditions specification options with the Precipitation-Runoff Modeling System (PRMS), U.S. Geological Survey Techniques and Methods, book 6, chap. 8, 60 p.
- Regan, R. S., Markstrom, S. L., Hay, L. E., Viger, R. J., Norton, P. A., Driscoll, J. M., LaFontaine, J. H. (2018) Description of the National Hydrologic Model for use with the Precipitation-Runoff Modeling System (PRMS), U.S. Geological Survey Techniques and Methods, book 6, chap B9, 38 p. <https://doi.org/10.3133/tm6B9>
- Rientjes, T. H. M., Muthuwatta, L. P., Bos, M. G., Booij, M. J., & Bhatti, H. A. (2013). Multi-variable calibration of a semi-distributed hydrological model using streamflow data and satellite-based evapotranspiration. *Journal of Hydrology*, 505, 276–290. <https://doi.org/10.1016/j.jhydrol.2013.10.006> [Accessed January 30, 2017].
- Riggs, G. A., & Hall, D. K. (2016). MODIS snow products collection 6 user guide. Retrieved from <https://nsidc.org/sites/nsidc.org/files/files/MODIS-snow-user-guide-C6.pdf>
- Rover, J., Wright, C. K., Euliss, N. H., Mushet, D. M., & Wylie, B. K. (2011). Classifying the hydrologic function of Prairie Potholes with remote sensing and GIS. *Wetlands*, 32(2), 319–327.
- Saltelli, A., Ratto, M., & Tarantola, S. (2006). Sensitivity analysis practices: Strategies for model-based inference. *Reliability Engineering & System Safety*, 91(10–11), 1109–1125. <https://doi.org/10.1016/j.res.2005.11.014>.
- Sanders, M. J., Markstrom, S. L., Regan, R. S., & Atkinson, R. D. (2017) Documentation of a daily mean stream temperature module—An enhancement to the Precipitation-Runoff Modeling System, U.S. Geological Survey Techniques and Methods 6-D4. <https://doi.org/10.3133/tm6D4>
- Santanello, J. A., Peters-Lidard, C. D., Garcia, M. E., Mocko, D. M., Tischler, M. A., Moran, M. S., & Thoma, D. P. (2007). Using remotely-sensed estimates of soil moisture to infer soil texture and hydraulic properties across a semi-arid watershed. *Remote Sensing of Environment*, 110(1), 79–97. <https://doi.org/10.1016/j.rse.2007.02.007> [Accessed January 27, 2017].
- Schaibly, J. H., & Shuler, K. E. (1973). Study of the sensitivity of coupled reaction systems to 9 uncertainties in rate coefficients. II Applications. *The Journal of Chemical Physics*, 59, 3879–3888.
- Shaw, D. A., Vanderkamp, G., Conly, F. M., Pietroniro, A., & Martz, L. (2012). The fill–spill hydrology of prairie wetland complexes during drought and deluge. *Hydrological Processes*, 26, 3147–3156. <https://doi.org/10.1002/hyp.8390> [Accessed January 30, 2017].
- Shook, K., Pomeroy, J., & van der Kamp, G. (2015). The transformation of frequency distributions of winter precipitation to spring streamflow probabilities in cold regions; case studies from the Canadian Prairies. *Journal of Hydrology*, 521, 395–409. <https://doi.org/10.1016/j.jhydrol.2014.12.014> [Accessed January 27, 2017].
- The Nature Conservancy (2009). Indicators of Hydrologic Alteration Version 7.1 User's Manual. <https://www.conservationgateway.org/Files/Pages/indicators-hydrologic-altaspx47.aspx>
- Thornton, P. E., Running, S. W., & White, M. A. (1997). Generating surfaces of daily meteorological variables over large regions of complex terrain.

- Journal of Hydrology*, 190(3–4), 214–251. [https://doi.org/10.1016/S0022-1694\(96\)03128-9](https://doi.org/10.1016/S0022-1694(96)03128-9) [Accessed February 11 2014].
- Thornton, P. E., Thornton, M. M., Mayer, B. W., Wilhelmi, N., Wei, Y., Devarakonda, R., & Cook, R. B. (2014) Daymet: Daily surface weather data on a 1-km grid for North America, Version 2, Oak Ridge National Laboratory Distributed Active Archive Center, Oak Ridge, Tennessee, USA, accessed March 1 (2016). <https://doi.org/10.3334/ORNLDAAAC/1219>
- Thorstensen, A., Nguyen, P., Hsu, K., & Sorooshian, S. (2016). Using densely distributed soil moisture observations for calibration of a hydrologic model. *Journal of Hydrometeorology*, 17, 571–590. <https://doi.org/10.1175/JHM-D-15-0071.1> [Accessed February 9, 2017].
- Tiner, R. W. (2003). Estimated extent of geographically isolated wetlands in selected areas of the United States. *Wetlands*, 23, 636–652. [https://doi.org/10.1672/0277-5212\(2003\)023%5B0636:EEOGIW%5D2.0.CO;2](https://doi.org/10.1672/0277-5212(2003)023%5B0636:EEOGIW%5D2.0.CO;2) [Accessed February 9, 2017].
- U.S. Environmental Protection Agency (2015). Connectivity of streams and wetlands to downstream waters: A review and synthesis of the scientific evidence (final report), U.S. Environmental Protection Agency, Washington, DC, EPA/600/R-14/475F. Retrieved from <https://cfpub.epa.gov/ncea/risk/recordisplay.cfm?deid=296414%26amp%3BCFID=74339910%26amp%3BCFTOKEN=71400295> [Accessed February 9, 2017].
- U.S. Geological Survey (2007–2014). National Hydrography Dataset available on the World Wide Web. Retrieved from <https://nhd.usgs.gov> [Accessed 7/2013].
- U.S. Geological Survey (2016). National Water Information System—Web interface. doi:10.5066/F7P55KJN [Accessed April 15, 2016].
- Vanderhoof, M. K., Alexander, L. C., & Todd, M. J. (2015). Temporal and spatial patterns of wetland extent influence variability of surface water connectivity in the Prairie Pothole Region, United States. *Landscape Ecology*, 31, 805–824.
- Vanderhoof, M. K., Christensen, J. R., & Alexander, L. C. (2016). Patterns and drivers for wetland connections in the Prairie Pothole Region, United States. *Wetlands Ecology and Management*. <https://doi.org/10.1007/s11273-016-9516-9>
- Viger, R., & Bock, A. R. (2014). GIS features of the Geospatial Fabric for National Hydrologic Modeling, U.S. Geological Survey, Denver, CO, USA. doi:10.5066/F7542KMD [Accessed March 1, 2016].
- Viger, R. J., Hay, L. E., Jones, J. W., & Buell, G. R. (2010) Effects of including surface depressions in the application of the Precipitation-Runoff Modeling System in the Upper Flint River Basin, Georgia, U.S. Geological Survey Scientific Investigations Report 2010–5062, 37 p. Retrieved from <https://pubs.er.usgs.gov/publication/sir20105062> [Accessed February 9, 2017].
- Viger, R. J., Hay, L. E., Markstrom, S. L., Jones, J. W., & Buell, G. R. (2011). Hydrologic effects of urbanization and climate change on the Flint River Basin, Georgia. *Earth Interactions*, 15(20), 1–25. <https://doi.org/10.1175/2010EI369.1> [Accessed February 9, 2017].
- Vining, K. C. (2002) Simulation of streamflow and wetland storage, Starkweather Coulee subbasin, North Dakota, water years 1981–98, U.S. Geological Survey Water Resources Investigations Report 02–4113, 33 p. Retrieved from <https://pubs.er.usgs.gov/publication/wri024113> [Accessed February 9, 2017].
- Wanders, N., Karssenberg, D., de Roo, A., de Jong, S. M., & Bierkens, M. F. P. (2014). The suitability of remotely sensed soil moisture for improving operational flood forecasting. *Hydrology and Earth System Sciences*, 18, 2343–2357. <https://doi.org/10.5194/hess-18-2343-2014> [Accessed January 27, 2017].
- Winter, T. C. (ed) (2003) Hydrological, chemical, and biological characteristics of a prairie pothole wetland complex under highly variable climate conditions: The Cottonwood Lake area, east-central North Dakota. U. S. Geological Survey Professional Paper 1675, 128 p. Retrieved from <https://pubs.er.usgs.gov/publication/pp1675> [Accessed February 2, 2017].
- Winter, T. C., & LaBaugh, J. W. (2003). Hydrologic considerations in defining isolated wetlands. *Wetlands*, 23(3), 532–540. [https://doi.org/10.1672/0277-5212\(2003\)023%5B0532:HCIDIW%5D2.0.CO;2](https://doi.org/10.1672/0277-5212(2003)023%5B0532:HCIDIW%5D2.0.CO;2) [Accessed January 27, 2017].
- Zamora, R. J., Clark, E. P., Rogers, E., Ek, M. B., & Lahmers, T. M. (2014). An examination of meteorological and soil moisture conditions in the Babocomari River Basin before the flood event of 23 July 2008. *Journal of Hydrometeorology*, 15(1), 243–260.
- Zhang, K., Kimball, J. S., Nemani, R. R., & Running, S. W. (2010). A continuous satellite-derived global record of land surface evapotranspiration from 1983–2006. *Water Resources Research*. <https://doi.org/10.1029/2009WR008800>

How to cite this article: Hay L, Norton P, Viger R, Markstrom S, Regan RS, Vanderhoof M. Modelling surface-water depression storage in a Prairie Pothole Region. *Hydrological Processes*. 2018;32:462–479. <https://doi.org/10.1002/hyp.11416>